Aguila-Leon, J.; Vargas-Salgado Carlos; Chiñas-Palacios, C.; Díaz-Bello, D. (2022). Energy Management Model for a Standalone Hybrid Microgrid Through a Particle Swarm Optimization and Artificial Neural Networks Approach. Energy Conversion and Management. 267:1-17. https://doi.org/10.1016/j.enconman.2022.115920

Energy Management Model for a Standalone Hybrid Microgrid through a Particle Swarm Optimization and Artificial Neural Networks Approach

Jesus Aguila-Leon[a,b], Carlos Vargas-Salgado[a,c*], Cristian Chiñas-Palacios[a,b], Dácil Díaz-Bello[a]

[a] *Instituto Universitario de Ingeniería Energética, Universitat Politècnica de València, València, España.*

b Departamento de Estudios del Agua y de la Energía, Centro Universitario de Tonalá de la Universidad de Guadalajara, Tonalá, México.

[c] *Departamento de Ingeniería Eléctrica, Universitat Politècnica de València, València, España.*

Abstract

Energy management systems are usually used to integrate different energy sources into a coordinated microgrid system. However, given the variability of renewable sources and the complexity of calculating renewable resource availability and managing energy, it is not easy to incorporate efficient energy management models in a microgrid. This work focuses on developing a methodology to incorporate optimized artificial networks into a self-adaptable energy management system to improve microgrids performance. The proposed model consists of a set of artificial neural networks organized into a cascade configuration. A Particle Swarm Optimization algorithm optimizes each artificial neural network; the proposed model aims to estimate and provide information to the energy management system. The model is implemented in MATLAB/Simulink environment and fed with experimental data. Correlation analysis of system variables between the different artificial neural networks is performed to validate the proposed model. Simulated tests are performed with scenarios using experimental data, and an analysis of the system's response is performed in terms of the root mean squared error and linear regression. The results showed that, compared to related works, the proposed model reduced errors by 59% and 56% for single and multiple-step prediction of energy parameter estimators. Regarding the fitness of the power estimator from the EMM for the test scenarios, an 0.1245 RMSE was obtained.

Keywords: Artificial Neural Network, Particle Swarm Optimization, AC Microgrid; Energy Management Model, Syngas Genset.

1. Introduction

In recent years, due to the previous decades, indiscriminate use of fossil fuels to obtain energy, the interest in the integration of generation technologies based on renewable energies in Hybrid Renewable Energy Systems (HRES) in the form of electric Microgrids (MGs) has taken more and more prominence [1] with the development of new technologies [2] towards sustainable energy generation systems [3]. However, the intermittent and unpredictable nature of renewable energy sources is a problem in ensuring the reliability of the renewable energy technologies [4]. To improve the performance, and therefore, the

* Corresponding author. e-mail address: carvarsa@upvnet.upv.es (C. Vargas-Salgado).

reliability of the MGs, various strategies can be implemented, from the optimization in their design and sizing to the development and implementation of Energy Management Models (EMM) [5] and Energy Management Systems (EMS) [6]. In addition to the variability of the availability of renewable energy sources, energy demand is also difficult to predict since it depends on each user's preferences, which increases the instability of the MG [7].

Efficiently managing the resources of the MG is a task of the EMS [8]. The EMSs can be classified into two main categories: centralized and decentralized [9]. Centralized EMS are based on a central controller within the microgrid, which, according to the received information and operating algorithms, can make decisions to manage energy flows in the microgrid [10]. Meanwhile, decentralized EMS are incorporated into decentralized control topologies, where droop control plays a vital role in managing the various energy sources and energy storage systems to establish energy flow policies into the microgrid [11].

Conventional EMS algorithms are based only on the energy balance of the MG. These methods are usually inefficient since they do not consider other inherent aspects of the complexity and nonlinearity of microgrids [12], such as estimations of the availability of resources, learning historical data of user energy demand, climate variability in the region as well as detailed characteristics of energy storage and backup systems, such as the SoC in battery banks or suitable parameters for configuration and operation of the MG subsystems.

Given the many variables involved, creating an exact mathematical model of the microgrid and its components to be integrated into an EMS is a highly complex task. An alternative to obtaining a model of the microgrid subsystems that allows its adaptation to an EMS is using metaheuristic algorithms [13]. Nature is a source of inspiration for developing modern metaheuristic algorithms; they mimic natural systems and phenomena and translate them into computational methods [14]. Metaheuristic algorithms are a powerful tool, which in the field of MG its application can be classified into the following categories: optimal design of components and systems [15], optimal sizing [16], optimal control [17], prediction of resource availability [18], and energy management [19]. These categories can also be combined to obtain more reliable results [20].

Artificial neural network (ANN) algorithms are currently an interesting alternative for predictive modelling and control due to their robustness and handling capacity for complex non-linear relationships in dynamic systems, for example, in different applications in distributed Smart Grids (such as distributed energy management, generation forecasting, grid health monitoring, fault detection, etc.) [21] and load forecasting [22]. Those algorithms are based on biological neural network learning rules and procedures.

Since traditional approaches cannot solve the problems of hybrid energy systems due to the need of several energy sources and complexity, the use of ANN has lately arisen as a favourable tool because of their robustness and ability to deal with complex systems easily [23]. Artificial intelligence, such as ANN and bio-inspired algorithms, can improve the performance of hybrid microgrids in the energy management field.

Regarding the use of ANN for the optimum design of components and systems, several authors have performed improvements of MG systems using artificial neural network (ANN) algorithms, in [24] a hybrid model of an ANN with Particle Swarm Optimization (PSO) allowed the estimation of the power generated

by a Biomass Gasification Plant (BGP) in order to cover the energy demand in an experimental MG effectively. A dynamic voltage restorer (DVR) is applied in [25] by determining an ANN to protect sensitive loads from voltage disturbances.

Another example of ANN applied in renewable energy is shown in [26], where various ANN-based Maximum Power Point (MPP) tools are presented. The goal is to maximize the efficiency of photovoltaic panels, considering many electrical and environmental photovoltaic input parameters with six different scenarios. A total of six combinations were applied by the authors, combining electrical, thermal (Voc, Isc, FF) and environmental (RH, atmospheric pressure, PV back surface temperature, and irradiance information) parameters, outputs were validated by the root mean squared error (RMSE). Furthermore, in [33], for instance, models and designs the microgrid central controller upon the following rules applied to the energy management algorithm with the next priority sequence: first solar and wind sources, second biogas, then batteries, and lastly connection to the utility grid.

With respect to the use of ANN for achieving the optimal size of MGs, aiming to improve the performance of MGs, [28] uses a multiswarm spiral leader particle swarm optimization algorithm to identify the most relevant photovoltaic parameters to enable a good balance between exploration and exploitation mechanisms. The use of ANNs is also useful not only to analyze the performance of power exchange between generation sources in microgrids but also in terms of economics and emissions, [29] compares the operation of a ground source heat pump and a photovoltaic thermal system for a single house for heating and cooling purposes according to the time of the year from an ANN-based approach and a conventional on-off control.

Concerning the use of ANN for achieving the optimal control of MGs, authors in [30] conducted a study to assess the feasibility of ANNs and Nonlinear Autoregressive Exogenous (NARX) neural network models to model a fixed-bed downdraft gasification and to know the relation between the features of the gasifier and the regression performance. To achieve this, different feature groups were introduced: the first one consisted of the equivalence ratio (ER), airflow rate (AF), and temperature distribution; while the second one included biomasses value such as the equivalence ratio (ER), air flow rate (AF), and the reduction temperature. Thus, after comparing the NARX and ANN models, when using the temperature distribution as a feature, it is concluded that both methods are reliable, accurate, fast, and effective to control and optimize a woody biomass gasification process and thus syngas composition and calorific value.

Furthermore, [31] carried out two ANNs to adjust the power converters' pulses for the Voltage Source Inverter (VSI) used to control the DVR by regulating the voltage signals. Authors in [32] developed a microgrid central controller using embedded energy management algorithms for decision making at an isolated renewable energy system with the assistance of a multi-agent concept and multiple sensors at power sources, where sources like wind, solar, biogas, and batteries are considered. Besides, a connection to the utility grid in case of lack of energy from the microgrid and a power control mechanism for the operation of batteries is considered (with constraints such as: not to charge batteries above 80% of their State of Charge (SoC), and not discharge batteries below 20 % of their SoC).

Concerning the use of ANN to predict resource availability in MGs, in [33], the authors used an EMS based on stochastic optimization methods. The proposed model can reduce operating costs by defining a day-ahead operation and maximizing the use of renewable resources.

Regarding the question of power exchange between generation sources in a microgrid, bio-inspired algorithms have had an excellent performance related to the improvement of optimal energy production, such as [33], by forecasting the energy performance of a small scale photovoltaic/thermal system through PSO-ANN algorithms. In [29], it was shown that an adequate energy management system incorporating a Fuzzy Inference System (FIS) with a genetic algorithm (GA) helps maximize the benefit of energy exchange in the network. In addition, in [35] the same problem was addressed in a multi-microgrid environment by combining a Stackelberg game theory with a quasi-oppositional symbiotic organism search algorithm to improve energy exchange through a centralized MG controller incorporating a parallel fuzzy logic inference engine.

Other authors use different ANN tools for energy management in microgrids; an example is [36], which uses game theory, specifically canonical coalition games, to model an Energy Management System (EMS) to optimize the power exchange management in networked microgrids connected to the grid. Besides, not only one EMS, but a network of local EMS and a central EMS is proposed. Its main aim is to develop a power exchange strategy able to minimize transmission and transformation power losses with computational efficiency. To do so, a scheduled model is given to the canonical coalition game to generate a cooperative schedule for a changing horizon. The schedule generated is defined by each local EMS (of each microgrid), giving orders of the surplus or deficit power in each time.

Several authors have addressed the design of EMS with different approaches, intending to improve the performance of MG. Authors in [37] present a novel load management system for smart homes using neural networks and fuzzy logic for load classification; which achieves better scheduling of loads and an intelligent reduction in energy consumption, also adding layers of security to the system through metaheuristic techniques of cryptography. Similarly, [38] evaluates the performance of a cuckoo optimization algorithm of fuzzy controller and a PSO algorithm to optimize parameters in a hybrid power system.

As mentioned before, ANN are a powerful tool for forecasting, in [39] an EMMS is presented that makes use of a trained ANN with historical data on generation power, consumption and SoC of the microgrid, to determine the optimal mode of operation of the microgrid; while authors in [40] compare a proposed ANN-based backtracking search algorithm (ANN-BBSA) versus an ANN-based binary particle swarm optimization (ANN-BPSO) to limit fuel consumption, reduce CO_2 emissions and increase efficiency in a MG. Authors in [41,42] pay special attention to forecasting parameters, uncertainty, and demand response to increase MG reliability.

According to the literature consulted, the integration of metaheuristic algorithms to EMS follows various methodologies from author to author. The performance of metaheuristic algorithms, whether ANN or optimization algorithms, is strongly related to adjusting the parameters of these algorithms and the data with which they are fed. Nevertheless, there is still limited information regarding the modeling and validation of off-grid EMM systems from an ANN and PSO algorithms approach, with different scenarios of renewable energy availability and different conditions of the state of charge of the storage system. To

effectively manage the energy supply from a renewable base microgrid to a load, all this. In this work, a methodology for developing a model for an energy management model in small microgrids is presented. The proposed model incorporates a set of optimized neural networks in a cascade topology. The system can estimate the power output of the different generation sources to cover the energy demand, estimate the SoC of the battery bank and project the unserved energy, when applicable. The main contributions of this work are first to develop a new energy management model for a microgrid, incorporating a cascade configuration of ANN optimized employing PSO algorithms. Second to design and implement a methodology for analyzing the ANN outputs applied to MG, using correlation and linear regression matrices, and finally, to obtain an EMM capable of estimating the operating parameters of the ESS and a syngas-based generation backup unit to cover the energy demand in the MG optimally.

2. Method

The method followed to develop the proposed EMM is detailed in this section. First, the general architecture of the off-grid microgrid system is described, considering the power sources, storage system, and other components. Then, the proposed EMM explains how the neural network is integrated into the energy management system. Finally, the simulation conditions used for the model are detailed.

2.1 Microgrid architecture

The standalone microgrid consists of a PV array as the primary renewable source. When power generated by the PV array exceeds the load energy demand, energy is stored in a storage system. Additionally, a Biomass Gasification Plant (BGP) that feeds a Genset is available as a backup system. The microgrid architecture considered for the developed EMM is depicted in Figure 1.

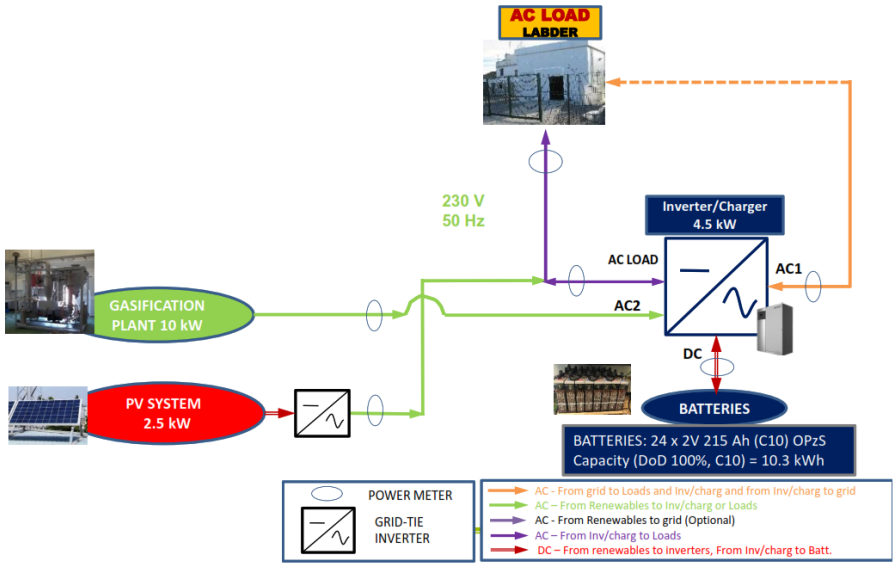

Figure 1 Overall architecture of the stan-alone microgrid for the proposed EMM.

As shown in Figure 1, the operation of the MG depends on a centralized controller. The proposed EMM objective is to use the produced energy efficiently, making preferential use of the cheapest sources, such as the PV system storage, and finally, the BGP to cover the user's energy demand. The main features of the microgrid are shown in Table 1. The Main components of the microgrid are shown in Figure 2.

Table 1 Microgrid main features for the proposed EMM.

Description	Main features
Photovoltaic array	2.1 kW, 12 solar panels BP7190S connected in series + Inverter Xantrex GT2.8-SP
Syngas production and power	10 kW @ 28 Nm3/h of Syngas and 13 kg/h biomass consumption.
Storage system	24 Batteries Sunlight 4 OPzS 200 in total 10,32 kWh storage capacity, 2 V @ 215 Ah batteries

a) ***b)*** ***c)***

Figure 2. Main components of the microgrid: a) PV system, b) storage system, c) Biomass gasification plant.

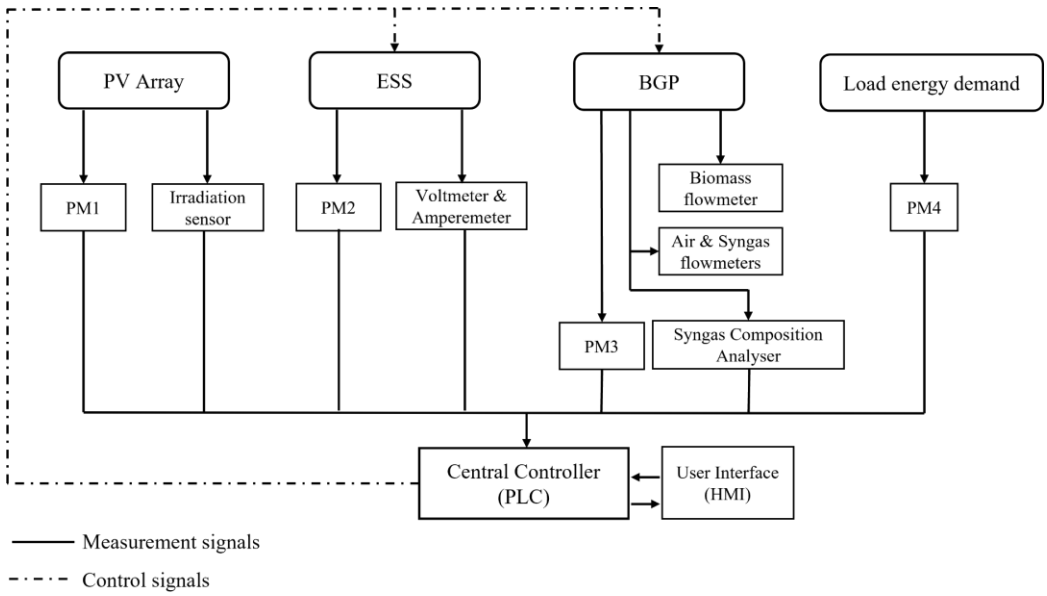

Figure 3. Control and measurement signals in the microgrid.

Table 2 Control system components.

Description	Device
Four power meters	Siemens Sentron PAC3200
Programmable Logic Device (PLC)	Omron CJ2M-CPU11
Programmable Logic Device (PLC)	Omron CP1L
Communication module	Omron CJ1W-SCU31
HMI touchscreen	Omron NS5-SQ10B-V2

Table 3 Measurement sensor and devices deployed in the microgrid.

Parameter	Units	Sensor	Measurement range
Solar irradiance	W/m^2	CEBEK C0121	0-1100 W/m^2; ±40 W/m^2
Air velocity	m/s	EE65 Series HVAC	0-20 m/s; ±0.4 m/s
Syngas flow meter	m/s	CTV-100	0-30 m/s; ±0.4 m/s
Gas analyzer	%	GASBOARD-3100P	0-100%; 0.01 %

The central controller receives information from the microgrid's sources and energy storage systems through sensors and Power Meters (PM) distributed in the microgrid. Since the primary goal of the EMM proposed in this research is to improve the energy management of the microgrid, collecting measurements of the electrical and environmental parameters is essential to make good decisions. For these purposes, several sensors and PM are deployed along the microgrid, as shown in Figure 3. The main components of the control system and measurement sensors are shown in Table 2 and Table 3, respectively.

One PM measures the energy produced by the PV system according to the incidence of solar irradiation measured by the CEBEK C0121 sensor. In addition to measuring the power delivered and received during the discharge and charge process in the storage system, since the DoD must be estimated, it is also essential to collect voltage and current data. When the PV power generation is insufficient to meet the energy demand and the energy stored in the battery is not enough, the BGP covers the energy demand. In the BGP, the energy generated is measured through another PM. The biomass flow to be gasified is measured through the conveyor RPMs, and a gas analyzer measures the composition of the syngas produced and estimates the Lower Heating Value (LHV). Finally, the airflow and the syngas going into the Genset are measured by flow meters. The main features of the BGP and its related Genset are shown in Table 4 andTable 5 Table 5.

Table 4 BGP main features.

Description	Feature
Gasification type	Bubbling fluidized bed
Biomass input @ 10%	5-13 kg
Biomass flow at power rating	10.5 kg/h
Efficiency	55-88%

Syngas production	10-28 Nm3/h

Table 5 Genset main features (Adapted from [43]***)***

Description	Feature
Brand	FG Wilson Generator
Model	UG14P1
Power rating	8.7 kW(syngas)
Velocity	1500 rpm
Compression ratio	8.5:1
Voltage and Frequency	230 V AC @ 50 Hz

The control and monitoring systems integrated in the microgrid and the EMM are shown in Figure 3.

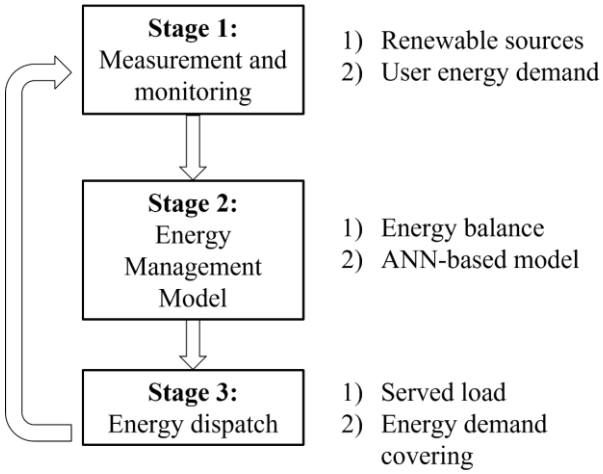

Figure 4 Workflow of the EMS in which ANN models are integrated.

The main objective of integrating the PSO algorithm with an ANN is to achieve a fast training algorithm for setting the weights and biases o the network. The PSO is constructed to train the NN model to accomplish a fast convergence rate and avoid getting trapped in a local minimum. The proposed model is validated by comparing it against some metaheuristic algorithms models found in the literature. Then, the model is tested to get the best results for the power energy generation in the microgrid.

The NN comprises a large number of neurons that are connected to solve a particular problem. It contains several layers, and each layer has a certain number of neurons. The output layer receives the information from the input layer, followed by the hidden layer. An activation function must trigger the output value, regularly expressed in boolean form. The output is computed based on the activation function method and the neuron data between the layers

The EMM proposed in this paper, as shown in Figure 4, integrates an ANN-based model for power backup. The model presented uses an ANN of the Cascade Forward Propagation (CF-P) optimized by the Particle Swarm Optimization (PSO) Algorithm. Figure 5 shows the inputs and outputs of the ANN used.

The implemented model has a recurrent cascade-forward topology. The ANN model is divided into three subnets:

- The first subnet inputs are the solar irradiation, the year's season, and time; The output is the PV array power generation.
- The second subnet is fed during day-time-hours, and the PV array power generation is estimated, on the one hand, by the first subnet, and on the other hand by the storage system power, the power demand, the current unserved energy, the frequency, and power factor as electrical parameters. The outputs of the second net are the energy demand to the BGP, the State of Charge (SoC) of the Energy Storage System (ESS), and the ESS power delivered
- In the third subnet, the inputs are the estimated energy demand to BGP, the SoC, and the ESS power delivered (estimated by the second subnet), the syngas composition, on the one hand. On the other hand, the frequency and the power factor are obtained as electrical parameters. The outputs are required biomass, syngas production, the airflow required in the Internal Combustion Engine (ICE), BGP power generated, and unserved energy, which is also an updated recurrent input to the previous subnet.

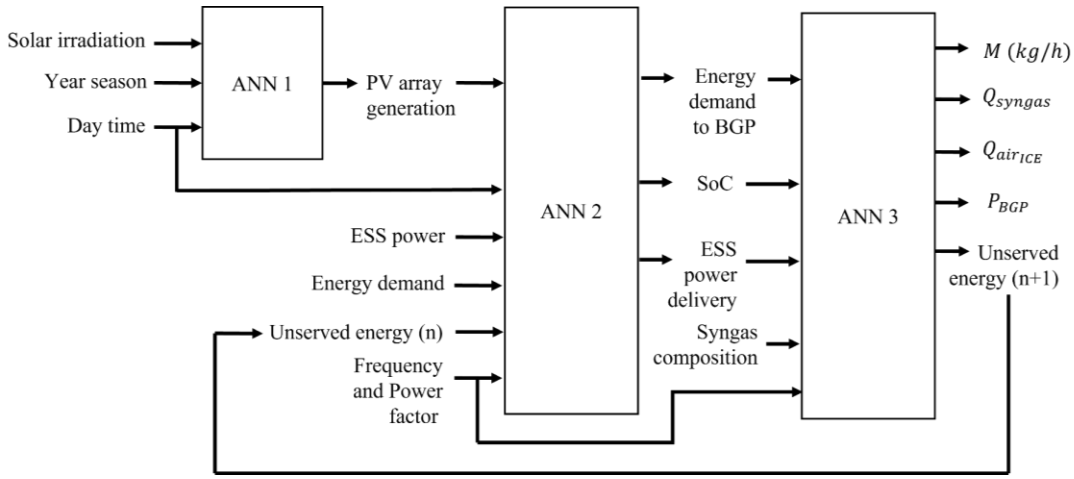

Figure 5. Artificial Neural estimation models inputs and outputs.

Before its use, the ANN is optimized by a PSO algorithm to find optimal values of weights and bias during the training. In this way, the error between the response of the real system and the predictions made by the model is reduced. The error between the actual response of the system and the response obtained by the prediction is measured in terms of the Mean-Squared Error (MSE). The PSO algorithm is based on the collective behaviour of animal species for survival by emulating the foraging mechanisms of various animal species, being a generalization of those survival strategies [44]. In this work, as mentioned before, the PSO algorithm is integrated as an optimizer for the ANN employed in the EMM. The integration of the PSO algorithm and the ANN to the EMM is shown in detail in Figure 6.

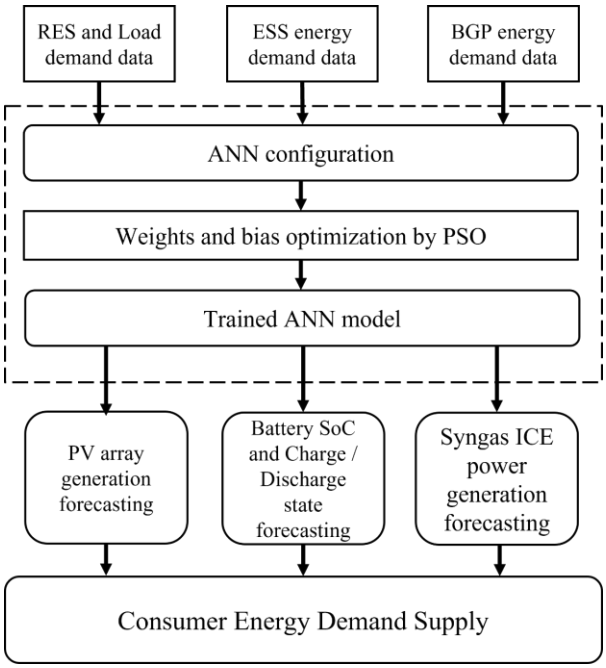

Figure 6 Integration of the ANN and the PSO algorithm to the proposed EMM.

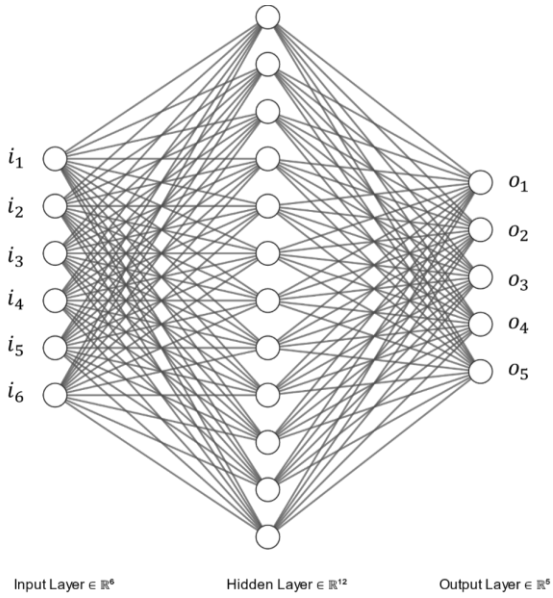

Figure 7. Overall structure of an ANN [45]**.**

Each entry signal to the ANN corresponds to a neuron of the input layer, as shown in Figure 7. A training process is necessary since the ANN simulates organic neurons' functioning. A series of data is fed into the ANN to learn and predict the system's output during the training process. As shown in Figure 7, each neuron of the input layer is interconnected to the neurons of the hidden layer, and these in turn to the neurons of the output layer. The vector $I_{ANN} = [i_1, i_2, \ldots, i_n]$ represents the inputs (every data fed into the set of ANN). As in nature, the neurons of the ANN are connected by links, and as the process of training and learning takes place, the strength of those links increases. The strength of the interconnection link is called weight, and the weight of the link between a neuron a and a neuron b is defined by $w(a, b)$. The propagation

function of the ANN is determined by equation (1) for each neuron of the input layer; the weighted sum transforms it in the activation functions (according to equation 2) for $n = 1$ to $n = 6$ in the next layer.

$$ANN_i = P_{fn_1}(o_{i_1}, o_{i_2}, \ldots, o_{i_n}, w_{i_1,j}, w_{i_2,j}, \ldots, w_{i_n,j}) \quad (1)$$

In equation (1) $o_{i_1}, o_{i_2}, \ldots, o_{i_n}$ are the output values of propagation function P_{fn_1}. In that sense, the activation function in the proposed ANN is defined by,

$$A_{fn_i}(t) = F_{act_i}(ANN_i(t), A_i(t-1), \phi_i) \quad (2)$$

Where the activation function is defined by F_{act_i} for each ANN used in the model, the n input in the network is A_{fn_i} and the activation status at the previous time is $A_i(t-1)$ for the i neuron. Once the ANN is ready, it is required to train it. The training aims to reduce the error between the output of the ANN and target values of evaluation. For this purpose, a proposed PSO algorithm has been integrated into the ANN to achieve better performance in ANN training by adjusting weights and bias during the training stage. Once the PSO algorithm is initialized, it randomly adjusts weights and biases in the ANN, and as the training iterations pass, these values are modified, according to specific previous parameters of the PSO, to reduce the MSE between the target values and the values predicted by the network. Each particle of the PSO algorithm corresponds to a different value of weights and bias in the ANN, which are adjusted in each iteration. These particles vary their position, velocity, and acceleration in the search space for possible optimal solutions. The optimal solution is considered to be one that meets the stop criteria requirements for the training algorithm and the PSO, either by the number of iterations and execution time or by the MSE error tolerance threshold. The vector W defines the optimization variables for the PSO algorithm according to equation (3) for k ANN, where *w* is the weight of each link between each pair of neurons i and j in the ANN. The number of variables of the optimization problem is *n*.

$$W_k = [w_{i_1,j}, w_{i2,j}, \ldots, w_{i_n,j}] \quad (3)$$

Each weight to be optimized is represented by $w_{i_n,j}$. Thus, the objective function of the PSO integrated into the proposed ANN for the EMM is defined by equation (4).

$$F_{min\,RMSE} \rightarrow \frac{\sum_{n=0}^{N}\left(o_{t_n} - o_{p_n}\right)^2}{N} \quad (4)$$

Where o_{t_n} is the target output value of the *n* data , o_{p_n} is the predicted output value of the same *n* data, and N is the total number of available training data. According to the definition of the PSO algorithm [46] in

each iteration, the particles find an optimal global solution called g_{best}. It is the best-obtained value of the objective function evaluated for each particle (of the total iterations made up to that moment). The best

tracking value for each particle is called best personal p_{best}. The speed update and the search for these optimal solutions (for each particle) is given by equation (5).

$$v_n = w * v_n + c_1 rand(x) * (g_{best,n} - x_n) + c_2 rand(x) * (p_{best,n} - x_n) \quad (5)$$

Where the n particle speed is determined by v_n, the inertia factor by w and the acceleration constants are represented by $c_1$and c_2.

2.2 Proposed Energy Management Model

The proposed EMM was designed to operate on an AC microgrid consisting of a photovoltaic solar array, a storage system, and a generation unit comprised of a BGP and a Genset. The MG controller works based on the MG subsystem outputs forecasted by a set of ANN related to each subsystem, then another ANN layer uses previous experience from the related experimental MG controller to execute the energy management for the MG. The election of the ANN and the optimization algorithm used in this research are based on the authors' previous work[23], where an optimized ANN-based model for a BGP is presented and compared against other traditional ANN models. Figure 8 shows the structure of the proposed EMM. The continuous lines represent the Energy flows, and the discontinuous ones are the communication bus.

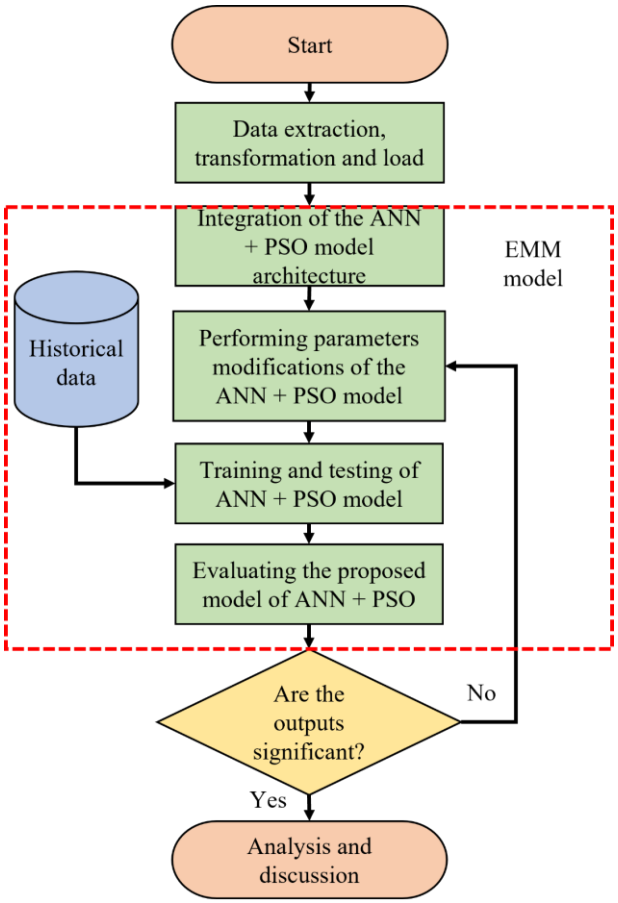

Figure 8 Overall structure of the proposed Energy Management Model.

As shown in Figure 8, the EMM is a central controller that collects information from the power generation and the backup sources and the energy consumption to be supplied. The flow of information between the EMM and the solar PV array is unidirectional. In contrast, the communication between EMM, the storage system, and BGP is bidirectional. In this case, the PV data information only sends solar irradiation and power generation data. The stages followed to design the proposed EMS are shown in Figure 9. The overall methodology is divided into three main stages.

As shown previously in Figure 9, Stage 1 collects data from the multiple energy generation and the ESS backup units. Data collected from the solar PV array are solar irradiation and power generation. This information is collected and transmitted to a central controller through a power meter (PM) and a solar cell. Data from the BGP is gathered by a set of the PM and gas, the airflow meters, and the gas analyzers to determine the syngas mixture composition used. The BGP acts as an energy backup source when the storage system runs out of energy, and there is an unsupplied amount of power from renewable sources. The BGP could cover the energy uncovered energy demand. When energy from renewable sources exceeds the energy demand, this energy is stored in the batteries. A PM measures the energy demand. The last operation in Stage 1 is for data filtering and conditioning to be sent to the central controller that operates accordingly to the proposed EMM.

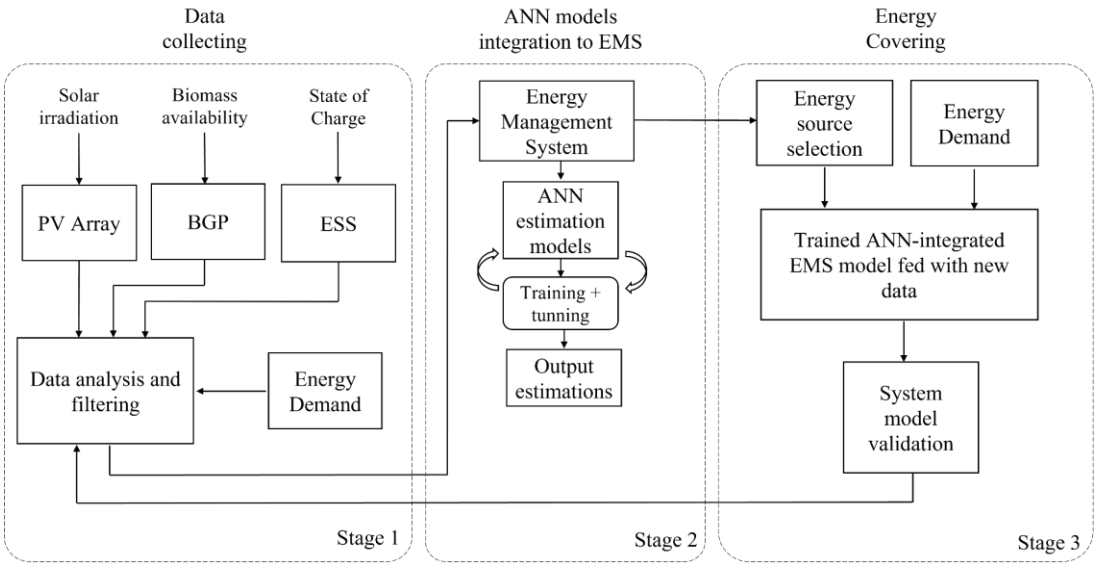

Figure 9 Overall methodology stages for integrating ANN models into the proposed EMS.

The proposed model uses input data for each ANN configuration. All the data used for the ANNs training are real collected during Stage 1, see Figure 9, measured based on instruments and sensors installed in the experimental microgrid of the Renewable Energy Laboratory (LabDER-UPV) of the Polytechnic University of Valencia detailed in the previous section. The data of solar irradiation, the PV array power, biomass consumption of the BGP as well as measurements of its operating parameters, measurements of voltages and currents and SoC of the battery bank, which were used for the training of the ANNs come from a set of experimental tests carried out throughout June 2019.

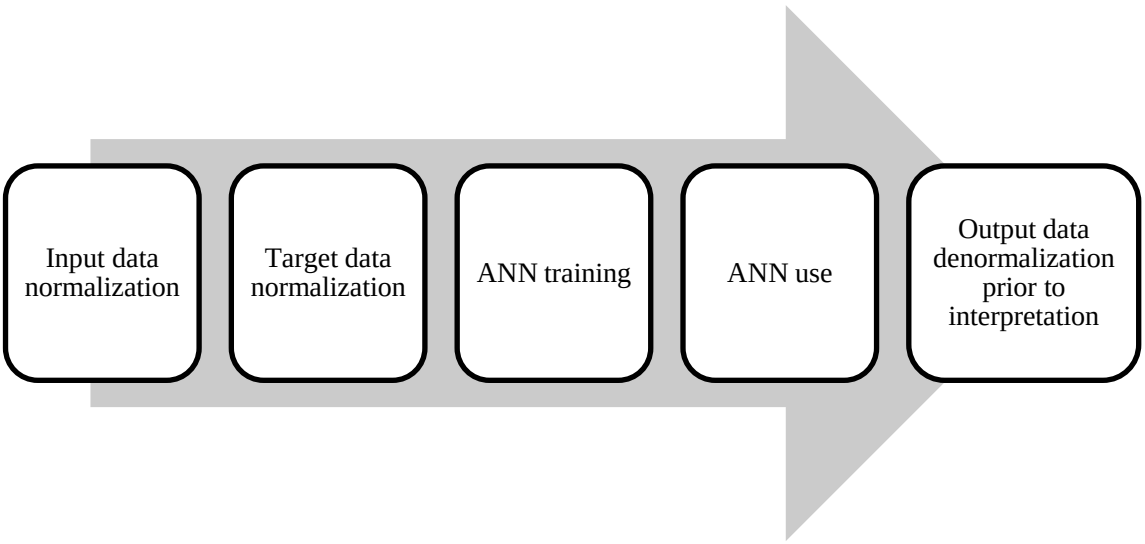

Figure 10. Training and use of a normalized-data ANN.

In the design of ANN, the normalization of the data is desirable to obtain better results. Normalization consists of adjusting the ranges of the ANN input values between [0,1] or [-1,1]. If the data is not normalized at the input, the ANN may have undesirable performance because not all network entries have a defined range of values; different values can be obtained in magnitude and reason change. Therefore, the optimal and desirable scenario is that all inputs and outputs are within a standard length range. The methodology for working on an ANN with standardized data is sown in Figure 10.

An ANN that has been trained with normalized data will deliver normalized data to its output, so once the results are obtained, these must be denormalized. The data transformation by the min-max normalization [47] defined by (6) for each input data, have been used in this work.

$$x'_i = (max_{scale} - min_{scale}) \cdot \left[\frac{(x_i - min_{val})}{(max_{val} - min_{val})}\right] + min_{scale} \quad (6)$$

Where,

x'_i is the i normalized input.

x_i is the i input.

max_{scale} is the maximum value of the range to be applied to the inputs.

min_{scale} is the minimum value of the range to be applied to the inputs.

max_{val} is the actual maximum value of the input dataset.

min_{val} is the actual minimum value of the input dataset.

To achieve uniformity in the training data, equation (6) was used with a value of 1 for max_{scale} and 0 for min_{scale}. All the magnitudes of the data were normalized on a scale of 0 to 1.

In Stage 2, all data are sent to the EMM of the MG central controller. The EMM can estimate the uncovered energy from the renewable energy sources and the storage system through an optimized Cascade Forward Propagation Artificial Neural Network (CFP-ANN), according to current environmental conditions the profile of the consumer load demand. The CFP-ANNs used for the EMM are optimized using a PSO algorithm to find the best combination of weights and bias during the CFP-ANN. The performance of the optimized ANN is evaluated in terms of the Mean Squared Error (MSE) and linear regression analysis. The main objective of Stage 2 is to estimate outputs of the proposed ANN-based model to predict uncovered energy from renewable sources and the storage system and the necessary biomass and airflow to produce syngas and generate power from the BGP to cover this energy deficit.

Finally, Stage 3 is set up for Energy Covering. The EMM uses the ANN output estimations to select the energy source in this stage. The off-grid MG balance of the total active power is expressed in (7).

$$P_{apc}(t) = P_{load}(t) - P_{PV}(t) - P_{ESS}(t) - P_{BGP}(t) \tag{7}$$

Where $P_{apc}(t)$ is the active power covered by the MG in off-grid operation mode, $P_{load}(t)$ is the energy demand, $P_{PV}(t)$ is the power delivered by the PV array, $P_{ESS}(t)$ is the power from the ESS, and $P_{BGP}(t)$ is the power coming from the BGP. The EMM constraint equations that define the operational limits are shown from (8) to (11).

$$-P_{PV\min} \le P_{PV}(t) \le P_{PV\max} \tag{8}$$

$$-P_{ESS\min} \le P_{ESS}(t) \le P_{ESS\max} \tag{9}$$

$$SoC_{\min} \le SoC(t) \le SoC_{\max} \tag{10}$$

$$-P_{BGP\min} \le P_{BGP}(t) \le P_{BGP\max} \tag{11}$$

Equation (8) denotes the constraints of the power obtained from the solar PV array, (9) to the output power of the storage system constraint, (10) to the storage system SoC constraint, and (11) the constraints of the power delivered by the BGP. The $P_{BGP}(t)$ power delivered by the BGP depends on the mixture of air and syngas in the electric generator and the heating value of the syngas, which in turn depends on its composition. All these considerations are integrated into the ANN involved in the proposed EMM. The energy source selection is executed by the EMM using a set of rules that consider the ANN predicted outputs. The EMM measurement and data flow are shown in Figure 11.

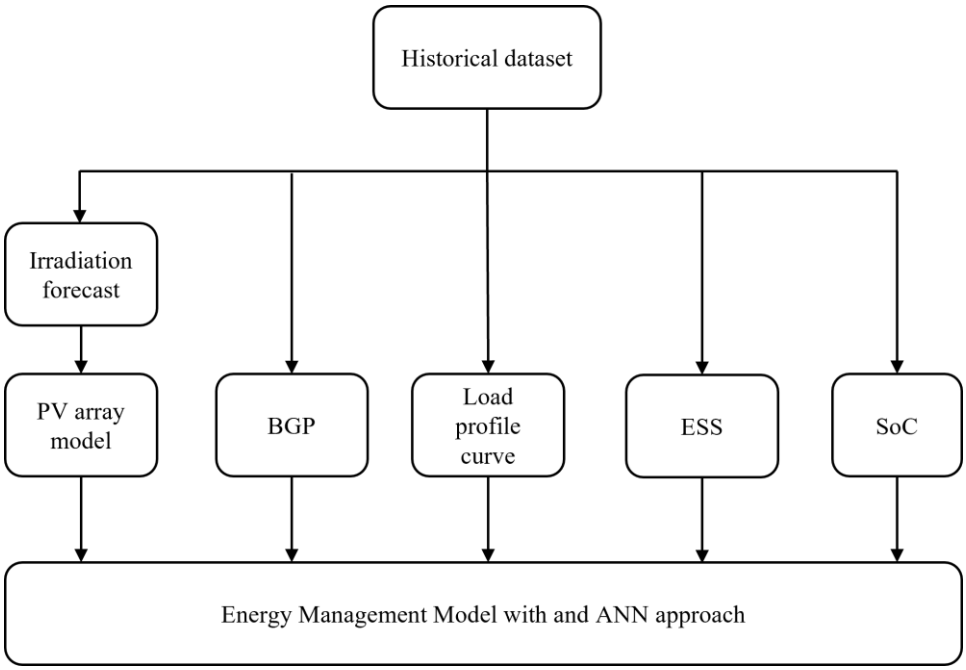

Figure 11. EMM measurement and data flow.

2.3 Simulation and Training

The proposed EMM was designed and implemented on MATLAB and Simulink, measured data from experimental tests of the microgrid located in the renewable energy laboratory of the Polytechnic University of Valencia were used to carry out simulations. Since the proposed model integrates ANN algorithms, a training phase is required. A total of 230,760 data were used for ANN training. Part of the TRAINING of the ANN consists of reducing the error between the outputs of the ANN and a set of objective values. To achieve this, the PSO algorithm was implemented to obtain the optimal values of weights and bias of the trained neural network. Table 6 shows the hardware used for the simulations, and Table 7 shows the ANN type and tuning parameters configured into the PSO algorithms.

Table 6. Hardware configuration of simulation platform for the proposed EMM.

Hardware	Characteristics
CPU	Intel Core i7-6700 @ 2.8 GHZ
RAM	16 GB DDR3 2133 MHZ
SSD	560 MBS / 520 MBS

Table 7. ANN and PSO parameters configuration for the proposed EMM.

Parameters	Adjust
Type of ANN	Feed -Forward Neural Network
Training algorithm	Particle Swarm Optimization
Population of particles	600

C1	2.5
C2	1.5
Function for performance	Mean Squared Error
Number of Input Neurons	6
Number of Hidden Layer	1-50
Number of Output Neurons	5
Learning Iterations	1000

The learning algorithm used in the ANN integrates the PSO, and to determine the error in the output of the ANN the MSE according to equation (12) was used.

$$MSE = \frac{1}{N}\sum_{n=1}^{N}\left(O_{predicted} - O_{target}\right)^2 \tag{12}$$

Where $O_{predicted}$ represents the output from the ANN and O_{target} is the target data taken from the experimental dataset, and N is the total number of samples.

Different simulation scenarios were used for various operating conditions in the microgrid, varying energy demand, and energy availability from sources. The validation of the proposed EMM was done for two cases, with different conditions of disposal of renewable energy in the MG and different conditions state of charge of the storage system. For both case studies, a standard demand curve was considered, typical of the application of MG taken as a model. In Table 8 can be seen the summary of the values of the storage system parameters used for each simulation under different environmental conditions.

Table 8 Value of initial parameters of the storage system.

Parameter	Value
Battery number	24
Roundtrip battery efficiency	90%
Battery nominal voltage	2 V
Battery capacity	210 Ah
Initial SoC	90%
Capacity (kWh)	10.1

Variable correlation

Prior to the simulation of the model, and its evaluation, it is important to perform a correlation analysis of the variables involved. Correlation is a statistical technique that allows to measure the level of relationship that exists between two or more variables [48], this allows to determine the level of interference that each variable has in each stage of the model.

There are several techniques for calculating correlation coefficients, within these methods are the Pearson Correlation, and the Spearman Correlation [49]. Pearson's method requires data to have a normal

distribution, while Spearman's method does not require this condition [50]. In the present work, the Anderson-Darling normality test method has been used, considering a p-value of significance of 0.05, to determine the normality of the variable dataset at each stage of the model. If the p-value of significance is less than 0.089 then the dataset is considered to have a normal distribution [51], and then Pearson's correlation method is applied.

Once the normality of the data has been determined and the correlation coefficients calculated, it is possible to perform a significance analysis between the variables. The correlation coefficient can have values from -1 to 1, determining the relationship strength between two or more variables as detailed in Table 9.

Table 9 Strength correlation coefficient interpretation.

From	To	Correlation strength
± 0.00	± 0.09	Null
± 0.10	± 0.19	Very weak
± 0.20	± 0.49	Weak
± 0.50	± 0.69	Moderate
± 0.70	± 0.84	Significant
± 0.85	± 0.95	Strong
± 0.96	±1.00	Perfect

A negative correlation coefficient indicates that the variables are related inversely, that is, when one variable has a high value the other has a low value, the closer to -1 the value of the correlation coefficient, the clearer the extreme covariance, and therefore a force of correlation, and covariance, very strong or perfect are obtained. When the correlation coefficient is equal or very close to zero, a null or a very weak correlation is obtained, so it is impossible to determine any sense of covariation between the variables. A strong or perfect positive correlation and covariance are obtained if the correlation coefficient is equal or very close to 1 positive.

3. Results

This section shows the main results of the paper. The results are divided in three subsections: Variable correlation analyst, ANN performance and EMM test.

3.1 Variable correlation analysis

Since the EMM proposed in this paper is based on a cascade model of ANNs, three covariance analyses have been performed for the variables involved in each of the three layers of the EMM. The first step in calculating the correlation coefficient between the variables in the model is to determine whether the dataset has a normal distribution, the results are detailed below.

Data normality test

To normalize the data, the Anderson-Darling Normality Test technique was used. It was determined that both the conjunct of data of the first, the second and the third layer have a normal distribution according to the criterion of the Anderson-Darling test, since all variables in all layers of the model have a p-value less than 0.05, so it is possible to perform a correlation analysis using Pearson's method.

Variable correlation analysis

Once it was found that the model variables follow a normal distribution, Pearson's method was applied to determine the correlation coefficients between each variable in each of the three layers of the EMM. The matrices obtained by the Pearson method for correlation coefficients are shown in Table 10 to

Table 12, for the first, second, and third layer of the EMM, respectively. In the tables mentioned, as the value of the correlation coefficient is closer to 1 it will be highlighted of a more intense green color, and the closer it is to -1 it will be highlighted in more intense blue color, for values close to 0 the color will be more subdued. The output variables of each EMM layer are highlighted in bold text.

Table 10 EMM first layer correlation coefficient matrix.

Coefficient	Hour	Irradiation	PV Gen.
Hour	1.00	-0.11	-0.12
Irradiation		1.00	0.98
PV Gen.			1.00

As shown in Table 11 above, the most significant variable for the generation of energy by the PV array is solar irradiation, considering the time window in which the data set was evaluated, so it has a low negative correlation coefficient value (-0.11). A perfect positive correlation between irradiation and power generation of the PV array was observed (0.98).

Table 11 EMM second layer correlation coefficient matrix.

Coefficient	PV Gen.	ESS power	Energy demand	Uns. Energy	Freq.	P.F.	E.D. BGP	SoC	ESS P. delivery
PV Gen.	1.00	0.06	-0.02	-0.33	-0.10	-0.10	-0.36	-0.18	0.09
ESS power		1.00	-0.14	-0.34	-0.66	-0.66	-0.54	0.50	0.99
Energy demand			1.00	0.65	0.54	0.54	0.78	-0.65	-0.18
Uns. Energy				1.00	0.50	0.51	0.77	-0.45	-0.37
Freq.					1.00	1.00	0.80	-0.89	-0.72
P.F.						1.00	0.80	-0.89	-0.72
E.D. BGP							1.00	-0.71	-0.59
SoC								1.00	0.55
ESS P. delivery									1.00

Table 12 EMM third layer correlation coefficient matrix

Coefficient	E.D. BGP	SoC	ESS P. delivery	CH_4 %	CO_2 ppm	CO %	H_2 %	N_2 ppm	Biomass Q	Syngas Q	Air Q	P. BGP	Uns. Energy
E.D. BGP	1.00	-0.71	-0.59	0.79	0.80	0.80	0.79	0.80	0.88	0.91	0.75	0.99	0.77
SoC		1.00	0.55	-0.88	-0.89	-0.89	-0.88	-0.89	-0.86	-0.77	-0.82	-0.75	-0.45
ESS P. delivery			1.00	-0.72	-0.72	-0.72	-0.72	-0.72	-0.70	-0.65	-0.67	-0.61	-0.37
CH_4 %				1.00	0.99	0.99	0.98	0.99	0.96	0.86	0.91	0.83	0.49
CO_2 ppm					1.00	1.00	0.99	1.00	0.96	0.87	0.92	0.84	0.50
CO %						1.00	0.99	1.00	0.96	0.87	0.92	0.83	0.52
H_2 %							1.00	0.99	0.96	0.86	0.92	0.83	0.51
N_2 ppm								1.00	0.97	0.87	0.92	0.84	0.51
Biomass Q									1.00	0.96	0.96	0.91	0.60
Syngas Q										1.00	0.93	0.92	0.65
Air Q											1.00	0.79	0.48
P. BGP												1.00	0.70
Uns. Energy													1.00

Thanks to the correlation matrix for the second layer of the EMM, shown in

As shown in Table 11 above, the most significant variable for the generation of energy by the PV array is solar irradiation, considering the time window in which the data set was evaluated, so it has a low negative correlation coefficient value (-0.11). A perfect positive correlation between irradiation and power generation of the PV array was observed (0.98).

Table 11, a covariance analysis can be performed between input variables and output variables.

For the output variable of the energy demand (ED) to the BGP strong positive correlation coefficients (cc) are observed with the electrical parameters such as frequency ($cc = 0.80$) and power factor ($cc = 0.80$) of the electrical signal as well as a significant cc with the energy demand ($cc = 0.78$); in addition to moderate negative correlation with the power delivered by the ESS ($cc = -0.59$) and a significant cc to its SoC ($cc = -0.71$). That means that the energy demand to the BGP depends directly on the energy to the MG, and its inverse to the ESS capacity and its SoC. Meanwhile, the SoC shows a moderate positive cc with the ESS power delivery ($cc = 0.55$), a moderate negative cc to the energy demand to the MG ($cc = -0.65$) and significant negative cc to ED to BPG ($cc = -0.71$). For the ESS power delivery, it depends on its actual capacity as can be constated with its $cc = 0.99$, and a moderate cc to the SoC ($cc = 0.55$).

As shown in Table 13 above, the correlation coefficient matrix for the third layer of the model has clearly delimited zones for very positive (close to 1) and very negative coefficients (close to -1). This gives an idea of the strong covariance, and therefore correlation, existing in each of the input and output variables in this model layer. All the output parameters of the BGP have a strong positive cc for the input variables, which mostly flow of biomass, air, syngas, and the composition of the syngas, which affects the calorific value of the same and therefore the amount of energy that can be extracted from it. While the output power of the

BGP is inversely proportional to the SoC and the capacity of the ESS as highlighted by the blue zones of the correlation coefficient matrix with moderate to significant negative cc values.

3.2 ANN performance

An EMM for an off-grid microgrid through particle swarm optimization and artificial neural networks approach was developed in this work to effectively manage the energy supply from a renewable base microgrid to a load. The proposed model considers as generation units a solar PV array and a BGP that operates as a backup. The PV array and the BGP can supply energy to the load or the storage system.

The integrated ANN EMM inputs are time, solar irradiation, load profile, calculated RES unserved power according to load demand, storage system power (input and output), syngas composition, frequency, and power factor. The predicted outputs are, on the one hand, the PV array generation, SoC, ESS charge/discharge power (according to the estimated power balance) and, on the other hand, from the BGP side are mass flow M, syngas flow Q_{syngas} and airflow $Q_{air_{ICE}}$. After the ANN estimations, the delivered power P_d and uncovered power P_u are calculated by the EMM, and the ANN outputs fed the EMM rules to manage the BGP operation inside the MG.

Table 13 Summary of MSE and linear regression of the trained ANN model.

Parameter	RMSE	R
Biomass flow (M)	0.0465	0.9944
Syngas generation$\left(Q_{syngas}\right)$	0.0393	0.9996
Airflow into the ICE $\left(Q_{air_{ICE}}\right)$	0.1194	0.9997
Power demand to BGP (P_d)	0.0513	0.9873
Power delivered by BGP(P_{SGPP})	0.0342	0.9810
PV array power generation $(PV_{Generation})$	0.0303	0.9871
Storage System State of Charge (SoC)	0.0419	0.9850
Storage System power delivery $\left(BB_{power}\right)$	0.0212	0.9960
Unserved energy prediction (P_u)	0.0513	0.9716

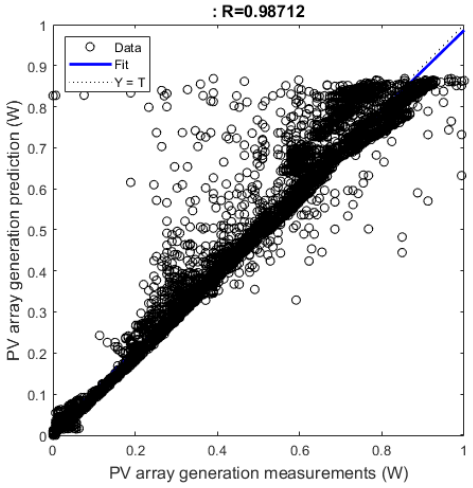

(a) PV generation prediction.

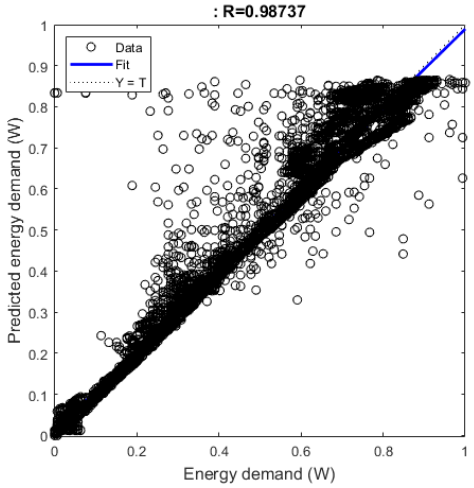

(b) Energy demand prediction.

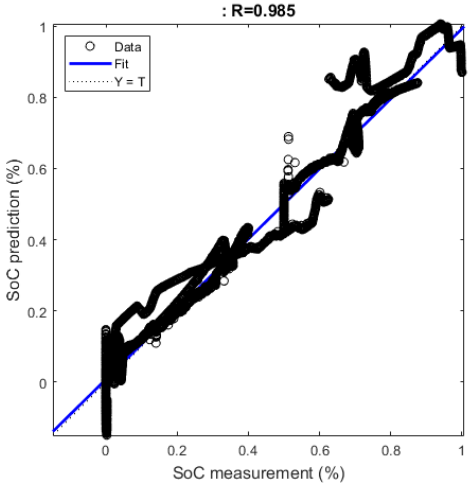

(c) SoC prediction.

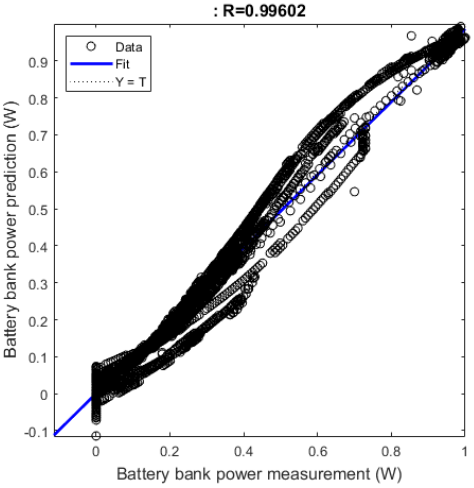

(d) SS power prediction.

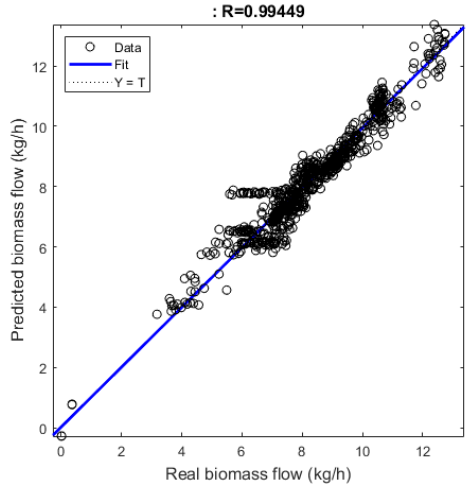

(e) Biomass flow prediction.

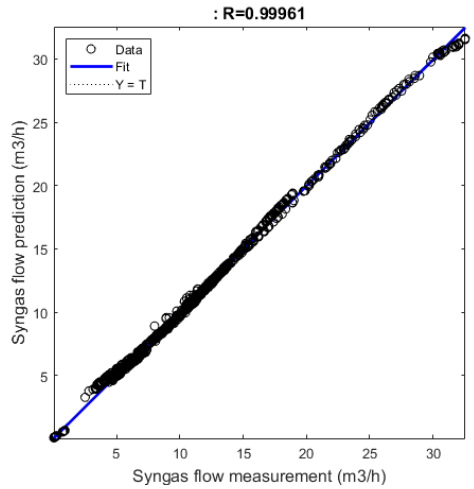

(f) Syngas flow prediction.

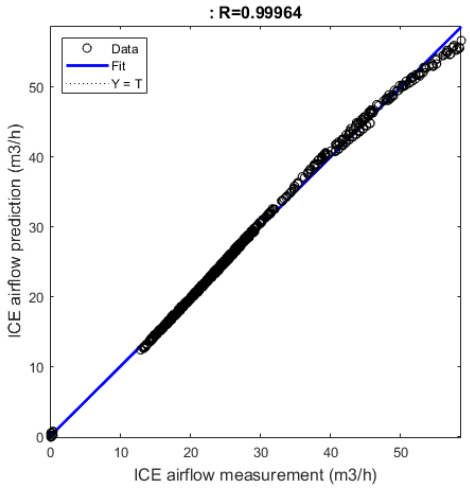

(g) ICE airflow prediction.

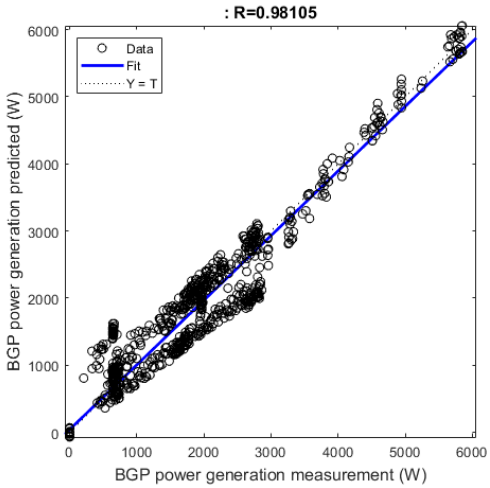

(h) BGP power generation prediction.

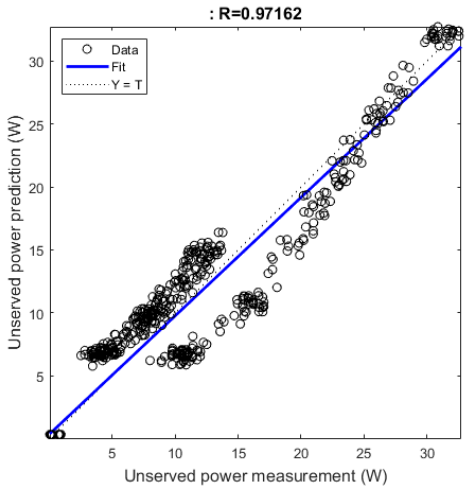

(i) Unserved power prediction.

Figure 12 Linear regression plots from the ANN model predicted parameters. (a) is the output of the first ANN layer, (b) to (d) are the outputs of the second ANN layer, and (e) to (i) are the third ANN layer outputs.

For the ANN training, a total of 480 simulations were carried out to find the best weight and bias configuration to predict the desired outputs from the ANN-based EMM using a 115,360 measurements dataset for each case. The summary of the best results of RMSE and the correlation coefficient R are shown in Table 13. The R value from the linear regression analysis for the ANN model output indicates the performance of the trained ANN for each variable. R and linear regression plot of the ANN for each layer obtained from the ANN-based model are shown in Figure 12.

Linear regression graphs of the training outcome of ANNs have characteristic shapes that depend on various factors. Among the factors that are related in their form and proximity to a value of R = 1 are the amount of data available for the training of the ANN and the strength of the relationship between the variables selected as input and output for the training stage. Figure 12 (a, and b) have very similar shapes because both output variables depend on a similar and periodic training data set. The greater the amount of data, the better linear regression is obtained at the output of the ANN, as well as the strength of the

relationship between the input and output variables, that is, the closer to 1 or -1 the correlation coefficient between them, depending on whether there is a direct or inversely proportional relationship between the variables, see Figure 12(d, f, and g) were R coefficient is higher than 0.99. When a set of variables is chosen as input, and most of them have a weak relation between them, then a worst linear regression will be, see Figure 12(a, b, c, h, and i).

In some cases, the linear regression plot can show a double, or diverse, tendency line, as shown in Figure 12(c, d, and i). In the SoC, Figure 12(c), prediction linear regression plot multiple tendencies are observed due to that only two of the nine involved variables have a moderate positive cc value, that is the ESS power delivery ($cc = 0.55$) and the ESS capacity ($cc = 0.50$), this causes the ANN of this layer to get confused on the output prediction, to avoid this undesired effects it is needed to consider more related variables that are often difficult to measure in experimental MG since they need specialized devices. The same analysis can be performed in Figure 12(d) for the ESS power predictions were the only positive cc are the ESS capacity (cc=0.99) and a moderate cc for the SoC ($cc = 0.55$). For the unserved energy prediction, Figure 12(i), the double tendency line of the linear regression can be explained since there are only two variables (out of 13) with positive correlation coefficients; in this case only the input variable of the energy demand to the BGP has a significant cc strength with $cc = 0.77$ and the BGP power generated with $cc = 0.70$.

3.3 EMM test

Once the EMM was designed, and an evaluation of its performance was carried out based on covariance analysis of variables and linear regression plots, it proceeded to test the model using real data to obtain estimations. The Figure 13 shows the diagram in Simulink that was used to model the systems, however, once the ANNs were trained, it was possible to use each subsystem of the microgrid as a multi-step prediction, as black box models. Using black box modeling has advantages over mathematical or virtual approximation models, since the output of the system is modeled in fusion of inputs by historical using the ANNs.

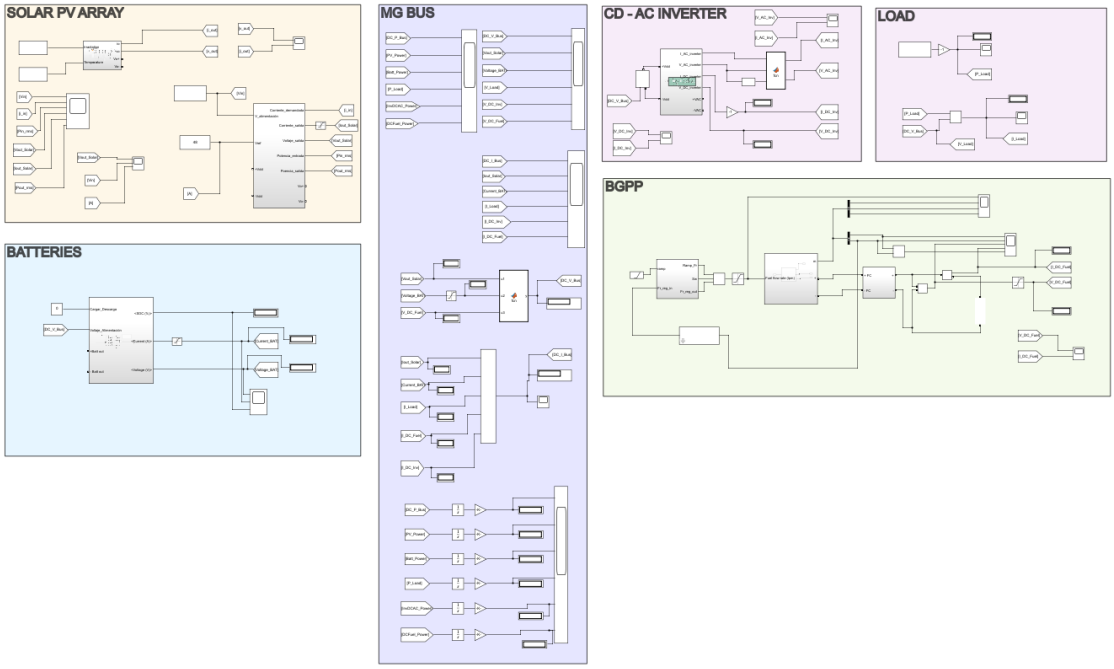

Figure 13 Simulink diagram of the AC microgrid.

The EMM was tested under two scenarios, a case 1 and a case 2, where the MG was tested under different environmental conditions. The load demand curve is shown in Figure 14. The load profile shown corresponds to the typical electrical consumption that the experimental MG covers during the week in the laboratory.

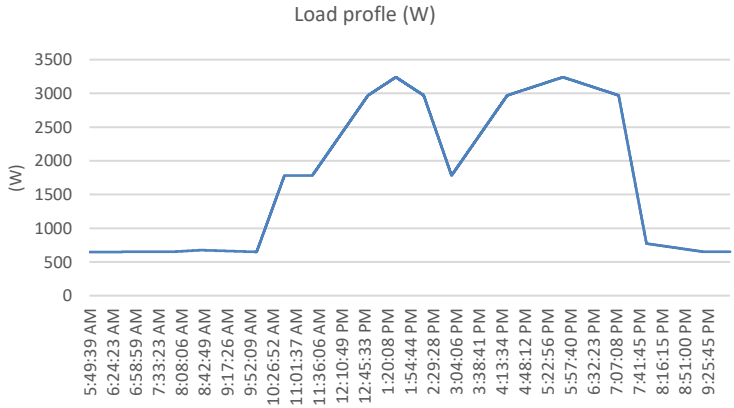

Figure 14 Typical load demand profile in the MG.

With the aim of stealing different scenarios for the EMM, the model was evaluated using different environmental, the consumption curve does not vary significantly throughout the week so the same curve has been used. Figure 15 shows the PV array outputs for case of study 1 and case of study 2.

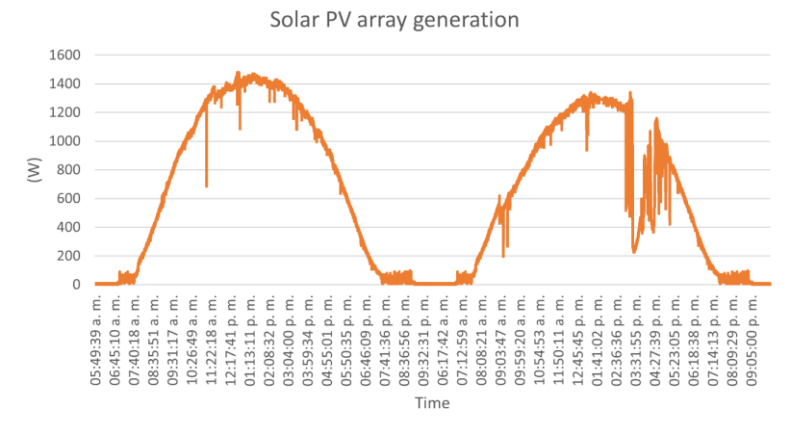

Figure 15 PV array outpus from cases of study.

The first part of the graph in Figure 15 corresponds to the power obtained by the PV array for the study case 1; the case study 2 PV array output profile corresponds to the second part of the graph in Figure 15. As can be seen, in case 2 there were greater variations in the solar irradiation that affected the solar panels, and therefore, the available RES energy availability causing the MG to operates under a more critical situation. The results obtained for the main parameters of interest are shown in the graphs in Figure 16.

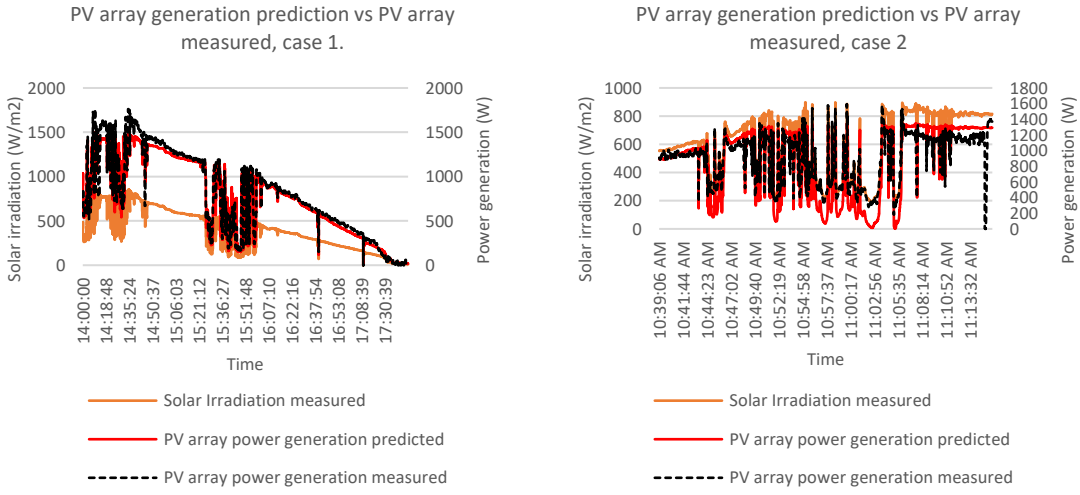

(a) *(b)*

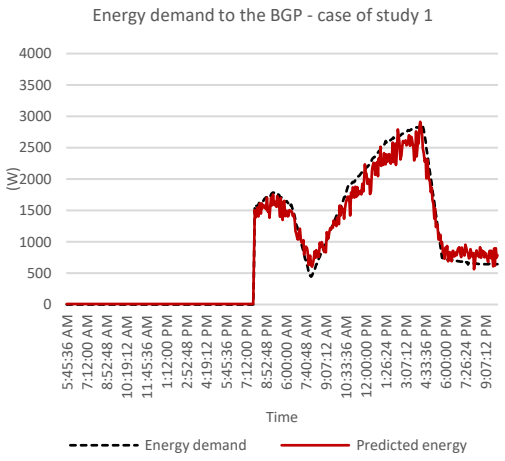
Energy demand to the BGP - case of study 1
(W)
Time
Energy demand
Predicted energy

(c)

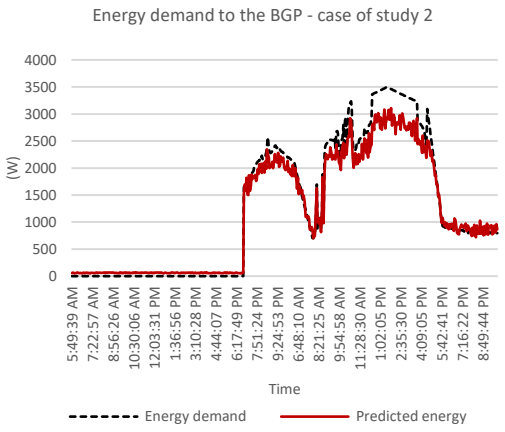
Energy demand to the BGP - case of study 2
(W)
Time
Energy demand
Predicted energy

(d)

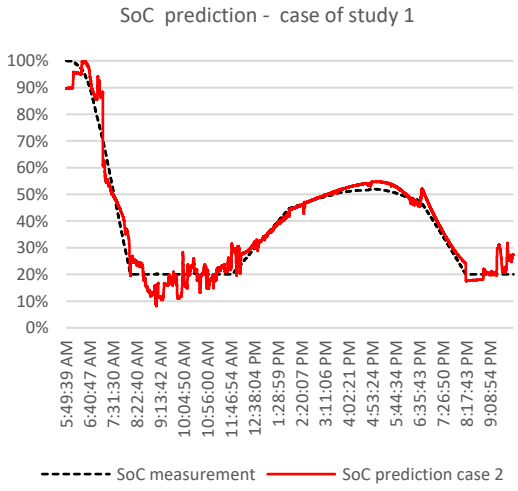
SoC prediction - case of study 1
SoC measurement
SoC prediction case 2

(e)

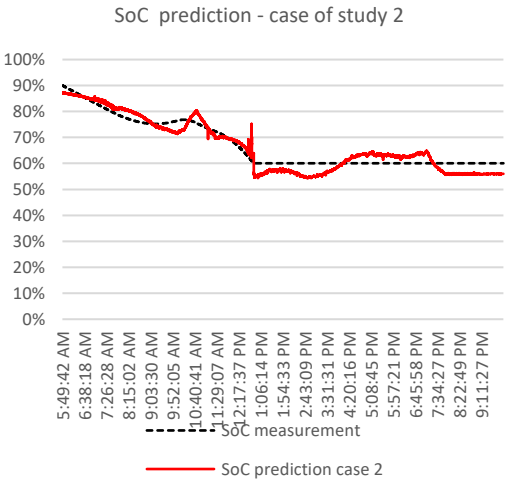
SoC prediction - case of study 2
SoC measurement
SoC prediction case 2

(f)

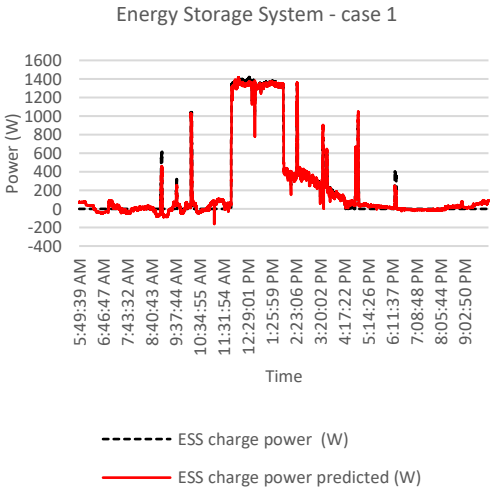
Energy Storage System - case 1
Power (W)
Time
ESS charge power (W)
ESS charge power predicted (W)

(g)

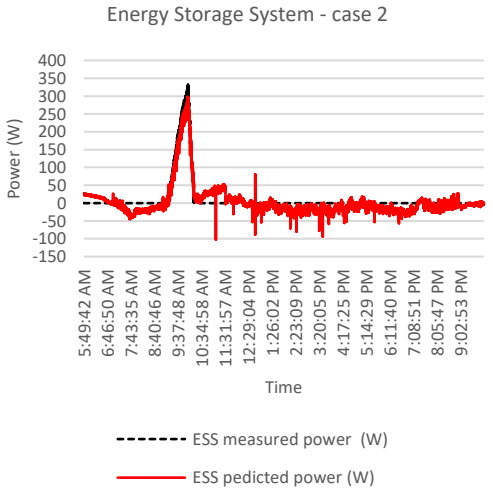
Energy Storage System - case 2
Power (W)
Time
ESS measured power (W)
ESS pedicted power (W)

(h)

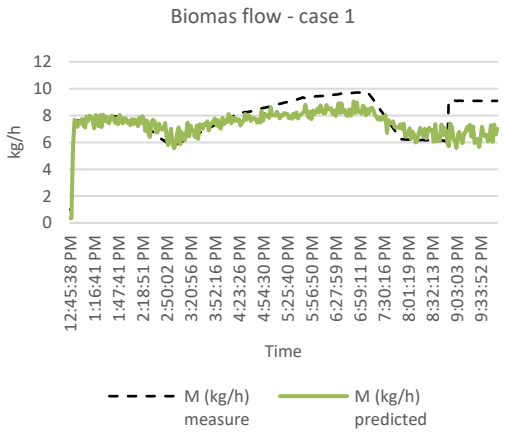

(i)

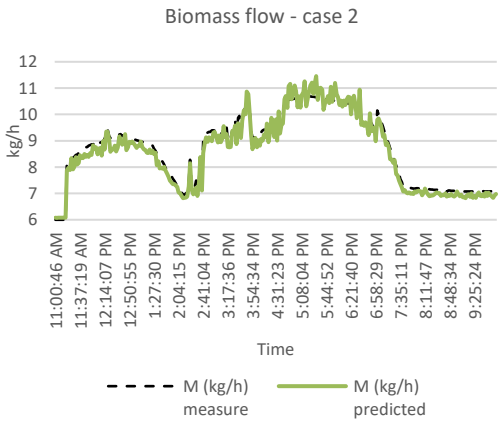

(j)

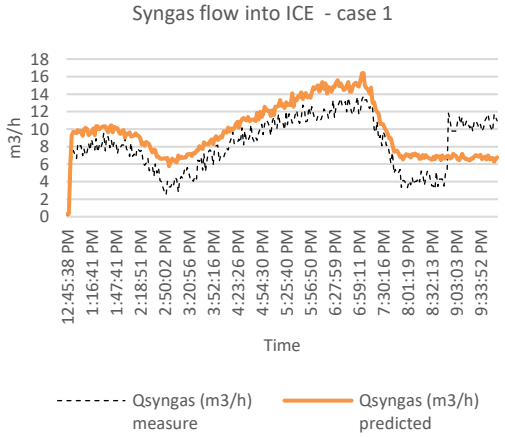

(k)

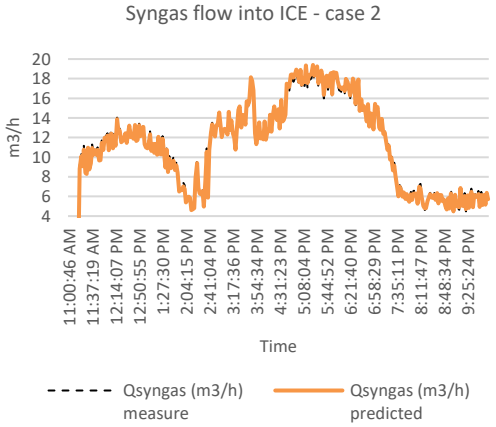

(l)

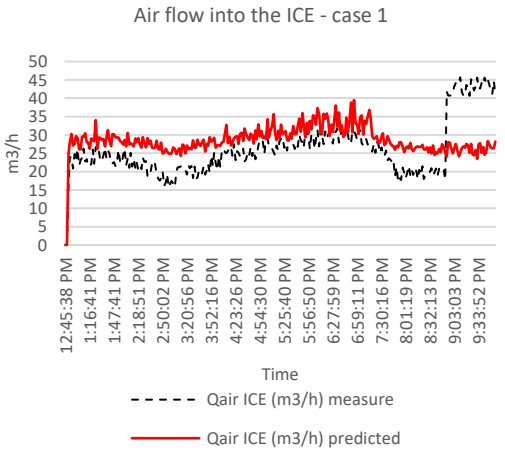

(m)

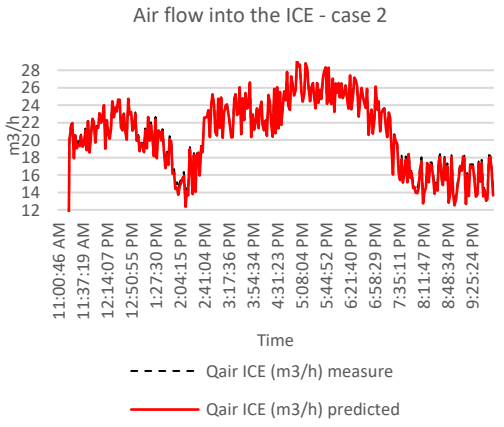

(n)

Figure 16 Plots of tests carried out for the EMM. In (a) and (b) the PV array generation for case 1 and 2 are shown. In (c) and (d) the Energy demand to BGP for case 1 and 2 are shown. In (e) and (f) the ESS SoC estimation for case 1 and 2 are shown. In (g) and (h) the ESS power for case 1 and 2 are shown. In (i) and (j) the Biomass flow to BGP

for case 1 and 2 are shown. In (k) and (l) the Syngas flow into the ICE for cases 1 and 2 are shown. And, in (m) and (n) the Airflow into the ICE for case 1 and 2 are shown.

As can been seen in Figure 16, in some cases there is a better fit between predicted and real data for case 2, this is caused due to that the EMM used for case 2 was also trained with case 1 data. In Table 14, a summary of the EMM performance indicators is shown.

Table 14 Summary of RMSE values from study case 1 and study case 2

	Case 1			Case 2		
	RMSE	R	MSD	RMSE	R	MSD
PV array generation	0.0303	0.9871	0.0159	0.0520	0.9871	0.0763
Energy demand to BGP	0.0513	0.9873	0.2085	0.0688	0.9873	0.2282
SS SoC	0.0419	0.9850	0.0210	0.0307	0.9850	0.0190
SS power	0.0277	0.9960	0.0139	0.0128	0.9960	0.0075
Biomass flow	0.2799	0.9944	0.4264	0.0443	0.9944	0.1609
Syngas flow	0.0583	0.9996	0.3503	0.0390	0.9996	0.1526
Air flow	0.9496	0.9997	4.5798	0.0585	0.9997	0.1786

As can be seen in Table 14, the EMM proposed in this work can estimate the main values of the EMS for an off-grid microgrid, for case 1 with which the model was tested, the lowest RMSE is in the estimation of the power in the ESS, being an RMSE of 0.0277, and the largest for the airflow with an RMSE of 0.9496, having the same behavior for the MSD, the lowest for the power of the batteries with a value of 0.0139 and the highest for the airflow. As for case 2, with which the EMM was tested; the lowest RMSE is equal for battery power with a value of 0.0128 and the highest RMSE of 0.0688 for energy demand for the BGP; in terms of the MSD, the same behavior is observed with a value of 0.0075 and 0.2282 respectively. Besides, the R values from the linear regression analysis for the ANN model output indicate the trained ANN's great performance for each variable, being the lowest R value 0.9871 for the PV array generation and the highest R value 0.9997 for the airflow.

Forecasting through artificial neural networks can be categorized as one-step prediction and multi-step prediction. When prediction is made using as input of an ANN only data measured it is called to be a one-step prediction, and when prediction is made using as input to ANN data that was previously output from another ANN it is called to be a multi-step prediction. In this research work, predictions of both types were used. In this work the prediction for the PV array output power is single step type; while prediction of biomass flow, syngas generation, airflow for the backup ICE, power demand to the BGP, power delivery from the BGPP, SoC of the storage system, power delivery of the storage system and unserved energy are multiple step prediction since they are related to the feed-forward cascade ANN topology implemented in the EMM. In the Table 15 is summarized the error from single step and multiple step predictions from the proposed model and compared to the results of other related works to estimate energy parameters.

Table 15 Comparison of RMSE from the EMM prediction to other related works using ANN to estimate energy parameters.

Prediction	Model	RMSE
Single step	Proposed EMM	0.0303
	[52]	0.0475
	[53]	0.1118
	[54]	0.0610
Multiple step	Proposed EMM	0.0506
	[55]	0.1174
	[56]	0.0751
	[57]	0.1492

As can be observed in Table 15, the average error reported in the literature consulted for variables of a single prediction step is 0.0734, while the error obtained by the EMM proposed in this work is 0.0303, achieving a reduction of 59% compared to other works. A reduction of 36% is achieved compared to [52], with respect to the work of [53] a reduction of 73%, and with respect to [54] a reduction of 50%. Regarding the multiple step predictions made by the EMM, the ANN network implemented in the model has an average error of 0.0506, while according to the models compared in Table 15, the average error is 0.1139, therefore, the model proposed in this work achieves a reduction of error by 56% compared to the average. Comparing the work of [55] a reduction of 57% is achieved, compared to the work of [56] a reduction of 33% and compared to the work of [57] a reduction of 66% in the RMSE error as a parameter index for the performance of the estimators.

4. Discussion and Conclusions

This work shows the results of the proposed EMM for a microgrid operating in off-grid mode, consisting of a PV solar array, an SS, and a BGP. The integration of an ANN in the dynamics model was tested to obtain the main parameter estimations of each subsystem. The primary objective of this proposed EMM was to increase the reliability and efficiency of the off-grid system, supplying energy to the load in case the RES and battery storage cannot meet that energy demand. Then the BGP must provide the required energy. The integrated cascade ANN architecture model consisted of a three-layer array of subnets; the last layer is recurrent to the second layer. The ANN model weights were optimized using the PSO algorithm. Once the model was created, the model's performance was validated by analyzing the model's output data. The output data were analyzed with an interpreted variable covariance study to determine the correlation coefficient matrices in each layer of the proposed EMM model and using linear regression graphs.

Regarding the covariance and correlation analysis, for the first layer of the EMM, a direct positive correlation was found between the irradiation and the output power of the PV array ($cc = 0.98$), with which the ANN obtained a very good performance as expected. In the second layer of the EMM both negative and positive correlation coefficients were found; this indicates that there are variables with covariance both

directly proportional and inversely proportional. In the third laayer of the EMM correlation coefficients with extreme values are obtained, that is to say, very high (close to 1) and very negative (close to -1); this indicates that there is a strong covariance and correlation between the inputs and outputs of the variables, and that the set of inputs used for the ANN operation are quite suitable for the prediction of results. However, in the case of the prediction of the SoC of the ESS, the ANN had particular difficulties in the prediction, this can be seen in the graph of the linear regression of the SoC, where various trends are appreciated, the analysis of the correlation matrix for this output variable indicates that of the input variables only one of 9 has a positive correlation coefficient and is not especially strong ($cc = 0.55$), which indicates that to improve the model it is necessary to achieve a new set of input variables with a correlation closer to the SoC to obtain a better prediction of it by the ANN of the EMM.

With respect to the ANN performance, on the one hand, it was evaluated using RMSE and linear regression graphs. The lowest the RMSE value the better, thus obtaining acceptable results, being between 0.1194 for the airflow into the ICE, and 0.0212 for the storage system power delivery. On the other hand, for the linear regression, the higher the values the close the ANN model designed is to reality, obtaining satisfactory values of between 0.9997 for the airflow into the ICE and 0.9716 for the unserved energy prediction.

After performing the analysis of the performance of the EMM, it was tested using real data and comparing with the prediction of the EMM before this data set, it was tested in two case studies varying the energy demand to the MG and the environmental conditions.

Two scenarios were evaluated. In the first scenario, the model obtained an RMSE of 0.2056 and MSD of 0.8023; in the second scenario, the RMSE was 0.0437 and an MSD of 0.1176. The reduction of the RMSE and the MSD between scenarios is explained due to the ANN learning capabilities; the second scenario was simulated using the first scenario's historical data to evaluate the improvement of the model as it is fed with more data, therefore the RMSE and MSD are significantly improved.

In short, the results of the evaluation of the performance show the reliability of the ANN-based EMM, since the average R coefficient was 0.9927 considering all subnets involved; meanwhile, the average RMSE was 0.1247, and the MSD of 0.4599. Moreover, the load coverage of the ANN-based EMM is satisfactory, as the unserved energy prediction has a low RMSE of 0.0513 and a high linear regression of 0.9716, quite close to the real system. In conclusion, using an ANN model built by three cascade subnets and with recurrence in the last layer is an effective alternative for the model of complex and dynamic electrical systems such as hybrid electric microgrids based on renewable energies, allowing the estimation of the main parameters that are used for energy management effectively.

The comparison made with worksof other authors who used ANN for one-step and multi-step prediction for estimation of electrical parameters in microgrid systems shows that the model presented in the methodology has a performance with a lower RMSE between 55% and 56% compared to the works consulted.

The present model shows a methodology that allows a validation of the model's performance in comparison to experimental data and the correlation of the variables involved in the multi-step prediction

processes for the parameter estimators within the MG as the performance index. This methodology may allow establishing a common frame for further developments

As future work, it is planned to improve the model for the integration of more generation and storage subsystems, continue training the ANN using more experimental datasets to obtain the most optimal solutions for the management of RES in MGs, as well as an automated control system for their management and optimization. Once the ANN has been completely developed, a study of energy savings and economic incomes of the optimized performance of the simulated microgrid could be calculated.

5. Acknowledgments

This study has been in part supported by the project: "Design Of a Hybrid Renewable Microgrid System" and "Microred Inteligente Hibrida de Energias Renovables para Solucionar el Trilema Agua-Alimentacion-Energia en Una Comunidad Rural de Honduras" ID 2020/ACDE/000306. The authors also express their sincere appreciation to Universitat Politènica de València for performing the proposed algorithm's tests and measurements at the Renewable Energies Laboratory (LabDER) at the Institute of Energy Engineering.

6. List of Acronyms

ANN	Artificial Neural Network
BGP	Biomass Gasification Plant
BP	Back Propagation
c_1	PSO particle personal acceleration coefficient
c_2	PSO particle social acceleration coefficient
cc	Correlation coefficient
CF-P	Cascade Forward Propagation
$CH_4[\%]$	Methane Percentage
CO_2	Carbon Dioxide
$CO_2[\%]$	Carbon Dioxide Percentage
CONACYT	Consejo Nacional de Ciencia y Tecnología
ΔP_{bed}	Fluidized bed pressure
E	Error
EBPGS	Energy Backup Power Generation Systems
EMM	Energy Management Model
EMS	Energy Management System
ESS	Energy Storage Systems
F	Frequency
F_{act_i}	ANN Activation Function
FF-BP	Feed Forward Back Propagation

FIS	Fuzzy Inference System
f_{min}	Objetive function to be minimized
F_{pro_n}	ANN Propagation Function
GA	Genetic Algorithm
Genset	Generator set (Generator + Alternator)
$H_2[\%]$	Hydrogen Percentage
HRES	Hybrid Renewable Energy Systems
LabDER-UPV	Renewable Energies Laboratory at the Universitat Politènica de València
LHV	Lower Heating Value
ICE	Internal Combustion Engine
M	Biomass flow
MG	Microgrids
MLP	Multilayer-Perceptron
MSD	Mean standard deviation
MSE	Mean Squared Error
N	Number of samples
N_2	Nitrogen Percentage
o_{i_j}	ANN weighted output
$o_{predicted}$	Predicted Output
o_{target}	Target Output
P	Active Power
PF	Power Factor
PSO	Particle Swarm Optimization
PV	Photovoltaic
$Q_{air_{gasifier}}$	Reactor Airflow
$Q_{air_{ICE}}$	Internal Combustion Engine Airflow
Q_{syngas}	Syngas flow
R	Coefficient of determination
RBF	Radial Basis Function
RES	Renewable Energy Source
SS	Storage system
T_{env}	Environmental Temperature
T_1	Gassifier inlet temperature
TEG	Hybrid Thermoelectric Generator
v_n	PSO particle velocity function
$w_{i_1,j}$	Neuron weight
WTG	Wind Turbine Generator

X_i	Optimization variables vector
$Y_{predicted}$	ANN output prediction
Y_{target}	ANN target training value

7. References

[1] Global Energy Review 2021 - Event - IEA n.d. https://www.iea.org/events/global-energy-review-2021 (accessed May 7, 2022).

[2] RENEWABLES_2018_GLOBAL_STATUS_REPORT n.d.

[3] Qazi A, Hussain F, Rahim NABD, Hardaker G, Alghazzawi D, Shaban K, et al. Towards Sustainable Energy: A Systematic Review of Renewable Energy Sources, Technologies, and Public Opinions. IEEE Access 2019;7:63837–51. https://doi.org/10.1109/ACCESS.2019.2906402.

[4] Mariam L, Basu M, Conlon MF. Microgrid: Architecture, policy and future trends. Renewable and Sustainable Energy Reviews 2016;64:477–89. https://doi.org/10.1016/j.rser.2016.06.037.

[5] Maurilio Raya-Armenta J, Bazmohammadi N, Gabriel Avina-Cervantes J, Saez D, Maurilio Raya-Armenta J, Sáez D, et al. Energy Management System Optimization in Islanded Microgrids: An Overview and Future Trends Maritime microgrids View project Coodinated Control and Management of Distributed Battery-Based Energy Storage Systems for Islanded Microgrids View project Highlights Energy Management System Optimization in Islanded Microgrids: An Overview and Future Trends Energy Management System Optimization in Islanded Microgrids: An Overview and Future Trends n.d. https://doi.org/10.13140/RG.2.2.11905.17769.

[6] Vera YEG, Dufo-López R, Bernal-Agustín JL. Energy management in microgrids with renewable energy sources: A literature review. Applied Sciences (Switzerland) 2019;9. https://doi.org/10.3390/app9183854.

[7] Mehdi Hakimi S, Hasankhani A, Shafie-khah M, Catalão JPS. Demand response method for smart microgrids considering high renewable energies penetration. Sustainable Energy, Grids and Networks 2020;21:100325. https://doi.org/10.1016/j.segan.2020.100325.

[8] Olatomiwa L, Mekhilef S, Ismail MS, Moghavvemi M. Energy management strategies in hybrid renewable energy systems: A review. Renewable and Sustainable Energy Reviews 2016;62:821–35. https://doi.org/10.1016/j.rser.2016.05.040.

[9] Rathor SK, Saxena D. Energy management system for smart grid : An overview and key issues 2020:1–43. https://doi.org/10.1002/er.4883.

[10] Fahad M, Elbouchikhi E, Benbouzid M. Microgrids energy management systems : A critical review on methods , solutions , and prospects. Applied Energy 2018;222:1033–55. https://doi.org/10.1016/j.apenergy.2018.04.103.

[11] Bukar AL, Tan CW, Said DM, Dobi AM, Ayop R, Alsharif A. Energy management strategy and capacity planning of an autonomous microgrid : Performance comparison of metaheuristic optimization searching techniques. Renewable Energy Focus 2022;40. https://doi.org/10.1016/j.ref.2021.11.004.

[12] Mirjalili S, Gandomi AH, Mirjalili SZ, Saremi S, Faris H, Mirjalili SM. Salp Swarm Algorithm: A bio-inspired optimizer for engineering design problems. Advances in Engineering Software 2017;114:163–91. https://doi.org/10.1016/j.advengsoft.2017.07.002.

[13] Rahmani R, Moser I, Cricenti AL. Modelling and optimisation of microgrid configuration for green data centres : A metaheuristic approach. Future Generation Computer Systems 2020;108:742–50. https://doi.org/10.1016/j.future.2020.03.013.

[14] Ashraf MA, Liu Z, Alizadeh A, Nojavan S, Jermsittiparsert K, Zhang D. Designing an optimized con fi guration for a hybrid PV / Diesel / Battery Energy System based on metaheuristics : A case study on Gobi Desert. Journal of Cleaner Production 2020;270:122467. https://doi.org/10.1016/j.jclepro.2020.122467.

[15] Rajamand S. Effective Control of Voltage and Frequency in Microgrid Using Adjustment of PID Coefficients by Metaheuristic Algorithms. IETE Journal of Research 2021;0:1–14. https://doi.org/10.1080/03772063.2020.1769509.

[16] Ma J, Ma X. A review of forecasting algorithms and energy management strategies for microgrids 2018;2583. https://doi.org/10.1080/21642583.2018.1480979.

[17] Singh AR;, Ding L, Raju DK, Seshu; KR, Raghav LP. Demand response of grid-connected microgrid based on metaheuristic optimization algorithm. Energy Sources, Part A: Recovery, Utilization, and Environmental Effects 2021. https://doi.org//10.1080/15567036.2021.1985654.

[18] Li G, Shi J. On comparing three artificial neural networks for wind speed forecasting. Applied Energy 2010;87:2313–20. https://doi.org/10.1016/j.apenergy.2009.12.013.

[19] Kazem HA. Evaluation of PV output in terms of environmental impact based on mathematical and artificial neural network models . International Journal of Energy Research 2021;45:396–412. https://doi.org/10.1002/er.5564.

[20] Rodríguez F, Fleetwood A, Galarza A, Fontán L. Predicting solar energy generation through artificial neural networks using weather forecasts for microgrid control. Renewable Energy 2018;126:855–64. https://doi.org/10.1016/j.renene.2018.03.070.

[21] Ali SS, Choi BJ. State-of-the-art artificial intelligence techniques for distributed smart grids: A review. Electronics (Switzerland) 2020;9:1–28. https://doi.org/10.3390/electronics9061030.

[22] Akhtaruzzaman M, Hasan MK, Kabir SR, Abdullah SNHS, Sadeq MJ, Hossain E. HSIC Bottleneck Based Distributed Deep Learning Model for Load Forecasting in Smart Grid with a Comprehensive Survey. IEEE Access 2020;8:222977–3008. https://doi.org/10.1109/ACCESS.2020.3040083.

[23] Laghari JA, Mokhlis H, Bakar AHA, Mohamad H. Application of computational intelligence techniques for load shedding in power systems: A review. Energy Conversion and Management 2013;75:130–40. https://doi.org/10.1016/j.enconman.2013.06.010.

[24] Chiñas-Palacios C, Vargas-Salgado C, Aguila-Leon J, Hurtado-Pérez E. A cascade hybrid PSO feed-forward neural network model of a biomass gasification plant for covering the energy demand in an AC microgrid. Energy Conversion and Management 2021;232. https://doi.org/10.1016/j.enconman.2021.113896.

[25] Sunny MSH, Hossain E, Ahmed M, Un-Noor F. Artificial Neural Network Based Dynamic Voltage Restorer for Improvement of Power Quality. 2018 IEEE Energy Conversion Congress and Exposition, ECCE 2018 2018:5565–72. https://doi.org/10.1109/ECCE.2018.8558470.

[26] Gowid S, Massoud A. A robust experimental-based artificial neural network approach for photovoltaic maximum power point identification considering electrical , thermal and meteorological impact. Alexandria Engineering Journal 2020. https://doi.org/10.1016/j.aej.2020.06.024.

[28] Nunes HGG, Silva PNC, Pombo JAN, Mariano SJPS, Calado MRA. Multiswarm spiral leader particle swarm optimisation algorithm for PV parameter identification. Energy Conversion and Management 2020;225. https://doi.org/10.1016/j.enconman.2020.113388.

[29] Roy K, Mandal KK, Mandal AC, Patra SN. Analysis of energy management in micro grid – A hybrid BFOA and ANN approach ARTICLE. Renewable and Sustainable Energy Reviews 2017. https://doi.org/10.1016/j.rser.2017.07.037.

[30] Yucel O. Comparison of the different artificial neural networks in prediction of biomass gasification products 2019:1–12. https://doi.org/10.1002/er.4682.

[31] Hassanein WS, Ahmed MM, Osama M, Ashmawy MG, Mosaad MI. Performance improvement of off-grid hybrid renewable energy system using dynamic voltage restorer. Alexandria Engineering Journal 2020;59:1567–81. https://doi.org/10.1016/j.aej.2020.03.037.

[32] Ahmadi SE, Rezaei N. Electrical Power and Energy Systems A new isolated renewable based multi microgrid optimal energy management system considering uncertainty and demand response. Electrical Power and Energy Systems 2020;118:105760. https://doi.org/10.1016/j.ijepes.2019.105760.

[33] Alnaqi AA, Moayedi H, Shahsavar A, Nguyen TK. Prediction of energetic performance of a building integrated photovoltaic/thermal system thorough artificial neural network and hybrid particle swarm optimization models. Energy Conversion and Management 2019;183:137–48. https://doi.org/10.1016/j.enconman.2019.01.005.

[35] Aguila-Leon J, Chiñas-Palacios C, Garcia EXM, Vargas-Salgado C. A multimicrogrid energy management model implementing an evolutionary game-theoretic approach. International Transactions on Electrical Energy Systems 2020;30:1–19. https://doi.org/10.1002/2050-7038.12617.

[36] Querini PL, Chiotti O, Fernádez E. Cooperative energy management system for networked microgrids. Sustainable Energy, Grids and Networks 2020;23:100371. https://doi.org/10.1016/j.segan.2020.100371.

[37] Chiñas-Palacios C, Aguila-Leon J, Vargas-Salgado C, Garcia EXM, Sotelo-Castañon J, Hurtado-Perez E. A smart residential security assisted load management system using hybrid cryptography. Sustainable Computing: Informatics and Systems 2021;32:100611. https://doi.org/10.1016/J.SUSCOM.2021.100611.

[38] Berrazouane S, Mohammedi K. Parameter optimization via cuckoo optimization algorithm of fuzzy controller for energy management of a hybrid power system. Energy Conversion and Management 2014;78:652–60. https://doi.org/10.1016/j.enconman.2013.11.018.

[39] Kang K, Choi B, Lee H, An C, Kim T, Lee Y, et al. Energy Management Method of Hybrid AC / DC Microgrid Using Artificial Neural Network 2021.

[40] Abdolrasol MGM, Hannan MA, Hussain SMS, Ustun TS, Sarker MR, Ker PJ. Energy Management Scheduling for Microgrids in the Virtual Power Plant System Using Artificial Neural Networks 2021.

[41] Hammid AT, Bin Sulaiman MH, Abdalla AN. Prediction of small hydropower plant power production in Himreen Lake dam (HLD) using artificial neural network. Alexandria Engineering Journal 2017. https://doi.org/10.1016/j.aej.2016.12.011.

[42] Tayab UB, Zia A, Yang F, Lu J, Kashif M. Short-term load forecasting for microgrid energy management system using hybrid HHO-FNN model with best-basis stationary wavelet packet transform. Energy 2020;203:117857. https://doi.org/10.1016/j.energy.2020.117857.

[43] Vargas-Salgado C, Aguila-Leon J, Chiñas-Palacios C, Hurtado-Perez E. Low-cost web-based Supervisory Control and Data Acquisition system for a microgrid testbed: A case study in design and implementation for academic and research applications. Heliyon 2019;5:e02474. https://doi.org/10.1016/j.heliyon.2019.e02474.

[44] Aguila-Leon J, Chiñas-Palacios C, Vargas-Salgado C, Hurtado-Perez E, Garcia EXM. Particle Swarm Optimization, Genetic Algorithm and Grey Wolf Optimizer Algorithms Performance Comparative for a DC-DC Boost Converter PID Controller. Advances in Science, Technology and Engineering Systems Journal 2021;6:619–25. https://doi.org/10.25046/aj060167.

[45] SVG N. Neural Network Design 2021. https://alexlenail.me/NN-SVG/index.html (accessed December 9, 2021).

[46] Chao O, Weixing L. Comparison between PSO and GA for parameters optimization of PID controller. 2006 IEEE International Conference on Mechatronics and Automation, ICMA 2006 2006;2006:2471–5. https://doi.org/10.1109/ICMA.2006.257739.

[47] Akanbi OA;, Amiri IS;, Fazeldehkordi E. A Machine-Learning Approach to Phishing Detection and Defense, 2015, p. 45–54. https://doi.org/10.1016/B978-0-12-802927-5/00004-6.

[48] Crawford SL. Statistical Primer for Cardiovascular Research Correlation and Regression 2006:2083–8. https://doi.org/10.1161/CIRCULATIONAHA.105.586495.

[49] Hauke J, Tomasz K. Comparison of values of pearson's and spearman's correlation coefficients on the same set of data. QUAESTIONES GEOGRAPHICAE 2011;30:87–93. https://doi.org/10.2478/v10117-011-0021-1.

[50] Myers L, Sirois MJ. Spearman Correlation Coefficients, Differences between. Encyclopedia of Statistical Sciences 2006. https://doi.org/10.1002/0471667196.ESS5050.PUB2.

[51] Minitab. The Anderson-Darling Statistic. Minitab 18 2019. https://support.minitab.com/en-us/minitab/18/help-and-how-to/statistics/basic-statistics/supporting-topics/normality/the-anderson-darling-statistic/.

[52] Rodríguez F, Fleetwood A, Galarza A, Fontán L. Predicting solar energy generation through artificial neural networks using weather forecasts for microgrid control. Renewable Energy 2018;126:855–64. https://doi.org/10.1016/J.RENENE.2018.03.070.

[53] Zhen H, Niu D, Wang K, Shi Y, Ji Z, Xu X. Photovoltaic power forecasting based on GA improved Bi-LSTM in microgrid without meteorological information. Energy 2021;231:120908. https://doi.org/10.1016/J.ENERGY.2021.120908.

[54] Ali Z, Putrus G, Marzband M, Tookanlou MB, Saleem K, Ray PK, et al. Online Sensorless Solar Power Forecasting for Microgrid Control and Automation. 2021 International Symposium of Asian Control Association on Intelligent Robotics and Industrial Automation, IRIA 2021 2021:443–8. https://doi.org/10.1109/IRIA53009.2021.9588690.

[55] Kuo PH, Huang CJ. A High Precision Artificial Neural Networks Model for Short-Term Energy Load Forecasting. Energies 2018, Vol 11, Page 213 2018;11:213. https://doi.org/10.3390/EN11010213.

[56] Rosato A, Panella M, Araneo R, Andreotti A. A Neural Network Based Prediction System of Distributed Generation for the Management of Microgrids. IEEE Transactions on Industry Applications 2019;55:7092–102. https://doi.org/10.1109/TIA.2019.2916758.

[57] Polimeni S, Nespoli A, Leva S, Valenti G, Manzolini G. Implementation of Different PV Forecast Approaches in a MultiGood MicroGrid: Modeling and Experimental Results. Processes 2021, Vol 9, Page 323 2021;9:323. https://doi.org/10.3390/PR9020323.